Published in final edited form as:

Mol Cancer Res. 2016 September ; 14(9): 869–882. doi:10.1158/1541-7786.MCR-16-0007.

FAK Expression, Not Kinase Activity, is a Key Mediator of Thyroid Tumorigenesis and Pro-tumorigenic Processes

Brittelle E. Kessler[1], **Vibha Sharma**[1], **Qiong Zhou**[1], **Xia Jing**[1], **Laura A. Pike**[1], **Anna A. Kerege**[1], **Sharon B. Sams**[2,3], and **Rebecca E. Schweppe**[1,2,3]

[1]Division of Endocrinology, Metabolism, and Diabetes, Department of Medicine, University of Colorado School of Medicine, Aurora, Colorado 80045, USA

[2]Department of Pathology, Department of Medicine, University of Colorado School of Medicine, Aurora, Colorado, 80045, USA

[3]University of Colorado Cancer Center, University of Colorado School of Medicine, Aurora, Colorado, 80045, USA

Abstract

There are limited therapy options for advanced thyroid cancer, including papillary and anaplastic thyroid cancer (PTC and ATC). Focal Adhesion Kinase (FAK) regulates cell signaling by functioning as a scaffold and kinase. Previously we demonstrated that FAK is overexpressed and activated in thyroid cancer cells and human PTC clinical specimens. However, it remains unclear whether patients with advanced thyroid cancer will benefit from FAK inhibition. Therefore, the dual functions of FAK in mediating pro-tumorigenic processes and thyroid tumorigenesis were investigated. Evidence here shows that FAK expression predominantly regulates thyroid cancer cell growth, viability, and anchorage-independent growth. FAK inhibition, with PF-562,271 treatment, modestly reduced tumor volumes, while FAK depletion, through shRNA knockdown, significantly reduced tumor volumes *in vivo*. A role for FAK expression in tumor establishment was demonstrated in a model of PTC, where FAK knockdown tumors did not develop. FAK depletion also led to a significant decrease in overall metastatic burden. Interestingly, pretreatment with a FAK inhibitor resulted in a paradoxical increase in metastasis in a model of ATC, but decreased metastasis in a model of PTC. These data provide the first evidence that FAK expression is critical for the regulation of thyroid tumorigenic functions.

Keywords

Focal Adhesion Kinase (FAK); kinase; scaffold; invasion; metastasis

Corresponding Author: Rebecca E. Schweppe, Division of Endocrinology, Metabolism, and Diabetes, Department of Medicine, University of Colorado School of Medicine, 12801 E 17th Ave, #7103, MS 8106, Aurora, CO 80045. Phone: 303-724-3179; Fax: 303-724-3920; Rebecca.Schweppe@ucdenver.edu.

The authors declare no conflicts of interest.

INTRODUCTION

Thyroid cancer is the most common endocrine malignancy accounting for ~4% of all new cancer cases diagnosed in 2014 in the U.S. (1), and the incidence has been increasing (2). While the majority of patients respond well to standard-of-care therapy, including tumor resection and radioactive iodine, local recurrence occurs in up to 20% of patients (3). Patients with advanced thyroid cancer, including those diagnosed with advanced papillary thyroid cancer (PTC), anaplastic thyroid cancer (ATC), and those with distant metastases, have extremely reduced survival. Specifically, patients with advanced PTC have a 5-year survival rate of 55% while patients with ATC, accounting for the most thyroid cancer related deaths, have a 1-year survival rate of only 20% (2). Unfortunately, there are limited effective therapy options for these patients (4).

Approximately 70% of thyroid cancers exhibit aberrant activation of the Mitogen Activated Protein kinase (MAPK) pathway due to mutations in effector proteins, including B-Raf, Ras, and through RET/PTC rearrangements (4). Despite the importance of the MAPK pathway in thyroid cancer, MAPK-directed therapies have had limited efficacy thus far (2). We have focused on the role of Src family kinases (SFKs), which are frequently overexpressed and activated in many tumor types (5). Src has been shown to promote multiple pro-tumorigenic functions including proliferation, survival, and migration through activation of downstream pathways including phosphoinositide 3-kinase (PI3K), Stat-3, p130Cas, paxillin, and focal adhesion kinase (FAK) (6). FAK (PTK2) has been shown to physically and functionally interact with Src to promote a variety of cellular responses (7). Notably, our previous studies have shown that FAK phosphorylation at the Src-dependent phosphorylation site, Y861, correlates with Src inhibitor sensitivity in thyroid cancer cell lines *in vitro* and *in vivo* (8,9).

Pathological studies have shown that FAK expression is deregulated in a number of cancers, including breast, colon, ovarian, pancreas, prostate, and others (10). In a previous study, FAK protein was observed to be overexpressed in a subset of PTC and ATC samples and correlated to a more invasive phenotype (11,12). We recently demonstrated that FAK is overexpressed in thyroid cancer cell lines, and in 10 out of 10 human PTC samples tested (8). We further showed that FAK is phosphorylated at Y861 in 5 out of 10 PTC samples (8). Accordingly, a study by Michailidi et al observed FAK expression in 25 out of 45 (75%) PTC samples and in 1 of 2 (50%) ATC samples (13). Phosphorylation of FAK at Y861 was more frequent in malignant compared to benign samples, and in PTC compared to hyperplasia samples, further supporting a role for Src and FAK signaling in thyroid cancer (13).

FAK is a non-receptor tyrosine kinase, and is a key regulator of signaling pathways by functioning as a scaffold to facilitate protein-protein interactions, and as a kinase by phosphorylating multiple substrates. This dual-function protein allows for cross-talk between integrins and growth factor receptors to regulate cell proliferation, survival, migration, and invasion (14). Autophosphorylation of FAK at Y397 occurs upon association with integrins or growth factor receptors. This phosphorylation site creates a high-affinity binding site for SH2-domain containing proteins such as Src and PI3K (14), which is thought to lead to the phosphorylation of other FAK tyrosine residues, including Y576/577

located in the kinase domain, as well as Y407, Y861, and Y925, thereby creating binding sites for effector proteins of downstream pathways (15). FAK can signal to the MAP kinase and Akt pathways, however, it remains unclear how mutational activation of the MAP kinase and PI3K/Akt pathways affects FAK-dependent signaling (16,17). Finally, effector binding sites on FAK are found within the FERM domain and the proline-rich regions, which are important for paxillin and p130Cas binding to regulate cell motility, migration, and invasion (15). Taken together, it is becoming clear that FAK mediates multiple signaling pathways through both its kinase and scaffolding functions. Therefore, FAK may promote key pro-tumorigenic processes through distinct kinase-dependent and kinase-independent (scaffolding) mechanisms, and targeting these dual functions may provide new therapeutic strategies for cancer patients.

Several small molecule inhibitors targeting FAK kinase activity have been developed and evaluated in both pre-clinical models and clinical trials. Recently, a phase I clinical trial with the FAK kinase inhibitor PF-562,271 (Pfizer) (acquired by Verastem, now VS-6062) was completed in pancreatic cancer, squamous cell carcinoma, and castrate-resistant prostate cancer, where ~30% of patients demonstrated stable disease at first restaging imaging (18). Thus, providing support for further investigation of FAK as a promising therapeutic target. In addition, clinical trials with other FAK kinase inhibitors including GSK-2256098 (Glaxo Smith Kline) and two drugs from Verastem, VS-6063 and VS-4718, originally PF-04554878 and PND-1186 respectively, are ongoing in patients with advanced ovarian cancer, solid tumors, and metastatic non-hematological malignancies (19,20). As noted above, because FAK can function independently of its kinase activity (by acting as a scaffold for protein-protein interactions), drugs that only target the catalytic activity of FAK may not be sufficient to block regulation of kinase-independent pro-tumorigenic responses (21). As such, drugs that block the protein-protein interaction between effector proteins and FAK are currently being evaluated in pre-clinical models. These include small molecules that interrupt the interaction between FAK and VEGFR, IGFR-1, Mdm-2, and p53 (Cure FAKtor Pharmaceuticals) (19). Therefore, in order to effectively target FAK clinically, a better understanding of FAK signaling is needed. Here we define the role of FAK expression and kinase activity, and demonstrate that FAK expression, not kinase activity, plays a key role in regulating thyroid cancer establishment, progression, and metastasis.

MATERIALS AND METHODS

Cell culture

Human thyroid cancer cell lines BCPAP, 8505C, and Cal62 were provided by M. Santoro (Medical School, University of Naples Federico II, Naples, Italy). SW1736 and C643 cells were obtained from Dr. K. Ain (University of Kentucky, Lexington, KY) with permission from N. E. Heldin (University Hospital, Uppsala, Sweden). TPC1 cells were provided by S. Jhiang (Ohio State University, Columbus, OH). TJH11T and THJ16T cells were obtained from J. A. Copland (Mayo Clinic Comprehensive Cancer Center, Jacksonville, FL). Prior to use in experiments, cell lines were validated using short tandem repeat profiling using the Applied Biosystems Identifiler kit (#4322288) in the Barbara Davis Center BioResources Core Facility, Molecular Biology Unit, at the University of Colorado, or as previously

described (8). Cells were also tested for *Mycoplasma* contamination using Lonza Mycoalert system according to the manufacturer's directions prior to use. Cells were grown in RPMI (Invitrogen) containing 5% FBS (Hyclone) and maintained at 37°C in 5% CO_2. shRNA targeting human FAK (Sigma mission TRCN0000121318 and TRCN0000121319) and a scramble control (Sigma mission pLKO.1-puro, SHC002) were packaged for lentiviral delivery via HEK293T cells using Effectene Transfection reagent (Qiagen), according to manufacturer instructions. Short-term selection was achieved with puromycin. Transductions of shRNA targeting FAK and the scramble control were performed for each individual experiment. shFAK TRCN0000121318 (shFAK1) was used for all *in vivo* experiments.

Cellular growth assays

BCPAP cells (1×10^4) or 8505C cells (5×10^3) were treated with 1 μM PF-573,228 (Pfizer) or DMSO every 3 days for 6 days, and harvested with trypsin-EDTA. Viable cells were counted using a Beckman Coulter ViCell cell counter with trypan blue exclusion as previously described (8). For sulforhodamine B (SRB) assays, cells were plated as previously described (9) and treated with increasing concentrations of PF-573,228, as indicated.

Soft agar assay

Cells (1×10^4) were suspended in 0.35% agar with complete media and plated on a base layer of 0.6% agar (Difco Agar Noble, BD Biosciences). After 24 hours, cells were treated with vehicle (DMSO) or 1 μM PF-573,228. Media containing vehicle or drug was replenished every 3 days for a total of 20 days. Colonies were stained with nitroblue tetrazolium chloride (Amresco; 5 mg/ml) and incubated overnight at 37°C to develop the stain. Colonies were counted using ImageJ software.

Western blotting

Cells treated with the indicated doses of PF-573,228 or DMSO were harvested in CHAPS lysis buffer (10mM CHAPs, 50mM Tris (pH8.0), 150mM NaCl and 2mM EDTA) with 1× phosphatase and protease inhibitor cocktail (Roche). Protein lysates resolved on SDS-PAGE gels were transferred to Immobilon-FL membranes (Millipore) and incubated at 4°C overnight with the following antibodies: FAK, p130Cas (BD Bioscience); pY397FAK (Abcam); pY925FAK, PYK2, pY416Src, pY527Src Src, pY410p130Cas, ppERK 1/2, ERK 1/2, pS473Akt, pT308Akt, Akt, ppT180/Y182P38, P38 (Cell Signaling); pY861FAK, pS910FAK, pY402PYK2 (invitrogen); α-tubulin (CALBIOCHEM) diluted in 1:3 Odyssey® Blocking Buffer in TBST (LICOR). Blots were incubated with secondary goat anti-mouse or anti-rabbit IRDye-conjugated antibodies (LICOR), and proteins were imaged with the Odyssey CLx imager (LICOR).

Invasion assay

BCPAP (5×10^5) and 8505C cells (4×10^5) were starved in RPMI with 0.1% FBS and treated with PF-573,228 or DMSO at the indicated concentration. After 24 hours, cells were harvested and seeded in the upper chambers of Matrigel-coated transwells 24-well, 8 μM pore size; BD Biosciences) in 0.1% FBS RPMI with PF-573,228 or DMSO. RPMI with 10% FBS and PF-573,228 or DMSO was added to the lower chamber. Cells were allowed to

invade for 24-hours. Invading cells on the lower surface of the membrane were fixed with methanol for one minute and stained DAPI (3 μg/mL, Invitrogen). Nuclei were quantified in five microscope fields under 10× magnification using Image J software and a Nikon microscope.

Drug preparation and administration

For *in vitro* studies, PF-573,228 was prepared in DMSO. For *in vivo* studies, PF-562,271 (50mg/kg) was prepared for daily oral gavage (7 d/wk) in 5% w/v Gelucire 44/14 (Gattefossé) in MiliQ water. For the orthotopic murine model, mice were randomized for treatment on day 10 based on bioluminescence activity. In the metastatic model, mice received PF-562,271 or vehicle, starting 2 days before intracardiac injection (pre-treatment), or on day 8 following randomization (post-treatment). Both treatment approaches were continued throughout the experiment.

Animal studies

All animal studies were conducted in accordance with the animal protocol procedures approved by the Institutional Animal Care and Use Committee at the University of Colorado Denver. For the orthotopic murine model, BCPAP and 8505C cells (5×10^5 in 5 μL) engineered to express a luciferase-IRES-GFP plasmid were injected into the right thyroid lobe of athymic nude mice (Harlan: Athymic Nude-Foxn1^{nu}; female, 6–8 week old), as previously described (9,22). Tumor establishment and progression was measured weekly by detection of bioluminescence with the Xenogen IVIS200 system (Caliper) in the University of Colorado Cancer Center (UCCC) Small Animal Imaging Core. Bioluminescence activity (photons/s) was quantitated using the Living Image 2.60.1 software (Igor Corp). Minimum/maximum thresholds were normalized to compare images using the same scale. Final thyroid tumor size was measured with calipers and volume was calculated using the following formula for an ellipsoid-like shape: tumor volume = (length × width × height)*0.5236.

For the experimental metastasis murine model, athymic nude mice (Harlan: Athymic Nude-Foxn1^{nu}; female, 5-week old) received D-Luciferin (3 mg) via intraperitoneal injection, and 5 minutes later each mouse was anesthetized using isofluorane. BCPAP-luc-IRES-GFP cells or 8505C-luc-IRES-GFP cells (10^5 cells in 100 μL PBS) were injected into the left ventricle using a 26-gauge needle, as previously described (9). Successful injection into the left ventricle was monitored by the pulsatile flow of red blood into the needle hub indicating correct placement, and by whole body bioluminescence immediately following injection (1 minute images). Metastatic progression was monitored weekly by IVIS imaging. Mice were sacrificed if more than 20% body weight was lost, and based on moribund criteria. For ex vivo imaging, mice were injected with D-luciferin (3 mg/mouse) before necropsy. Tissues of interest were excised, placed in 6-well tissue culture plates containing D-luciferin in PBS, and imaged for 5 seconds to 2 minutes.

IHC staining and pathologist scores

Tumors were collected and fixed in 10% buffered-formalin. Samples were embedded in paraffin and sections were cut by the UCD Research Histology Shared Resource Core.

Sections were stained with hematoxylin and eosin according to a standardized protocol. Invasion was scored by a pathologist using the following criteria: 1 = Minimal: Rare focal superficial invasion; 2 = Mild: Multifocal superficial invasion; 3 = Moderate: deep invasion; 4 = Severe: Extensive deep invasion with visceral invasion. IHC staining for Ki67 (Invitrogen #180191Z; 1:100) was performed and scored as percent of positive cells. CD34 (Abcam ab81289; 1:500) staining was performed by the UCD Research Histology Shared Resource Core. Sections were examined under low magnification for representative areas of tumor. Three 20× fields were selected with the highest density of vessels. Vessels were counted and counts averaged to determine the mean vascular density (MVD). Phosphorylated Y397FAK (Abcam ab8298; 1:300) staining was performed and scored based on degree of expression (0 through 3).

Statistical analysis

Data show the mean of at least 3 independent experiments ± SD or SEM, as indicated. GraphPad Prism statistical software was used to perform the 2-tailed Student's t-test and for 2-way ANOVA analysis. Fold changes are calculated from mean values of each treatment group. For all statistical analyses, asterisks (*) indicates $p \leq 0.05$; ** = $p \leq 0.01$; *** = $p \leq 0.001$, **** = $p \leq 0.0001$ and n.s = not significant.

RESULTS

Inhibition of FAK kinase activity versus FAK expression differentially regulates growth

We have previously demonstrated that increased levels of FAK phosphorylation at the Src-dependent site, Y861 and the FAK autophosphorylation site, Y397, correlates with sensitivity to Src inhibition (8,9). To further define the role of FAK in thyroid cancer, we focused on cell lines with high (BCPAP) and low (8505C) sensitivity to Src inhibition, to specifically evaluate the kinase-dependent and –independent functions of FAK (8,9). To define the role of kinase activity, we used the FAK kinase inhibitor, PF-573,228, to selectively inhibit FAK kinase activity. Figure 1A shows that while treatment with 0.1 μM PF-573,228 has modest effects on pY397-FAK levels (~10–20% reduction), treatment with 1 μM PF-573,228 resulted in decreased levels of phospho-FAK (pY397) in both BCPAP and 8505C cells (~40–50% reduction) (Figure 1A). Of note, complete inhibition of phosphorylation at pY397FAK was not observed at 1 μM of PF-573,228, potentially due to continued phosphorylation of this site by upstream kinases, as previously observed in other tumor models (23–25). Additionally, no compensatory increase in the phosphorylation of the FAK-related kinase, PYK2, was observed in either cell line with PF-573,228 treatment (data not shown). We next evaluated the effects of FAK kinase inhibition on Src activity, which has been coupled to FAK activation in other cellular contexts. Interestingly, Src phosphorylation at the activating Y416 site or negative regulatory Y527 site was not affected by FAK kinase inhibition in either the BCPAP or 8505C cells (Figure 1A). Consistent with the lack of regulation of Src, we show that phosphorylation of the Src-dependent sites, Y861FAK and Y925FAK, are not altered in response to PF-573,228 treatment, indicating that Src-dependent phosphorylation of these sites is not disrupted by inhibition of FAK autophosphorylation (Figure 1A). Further evaluation of p130Cas, a downstream target of FAK and Src (26), showed no consistent regulation in response to PF-573,228 treatment

(Figure 1A). However, we have previously shown that phosphorylation of paxillin and p130Cas is inhibited in response to Src inhibition (9) (data not shown), indicating that p130Cas is a target of Src and not FAK. Together these results indicate that while inhibition of FAK kinase activity with PF-573,228 reduces FAK autophosphorylation, this does not disrupt the activity of Src, or the phosphorylation of the Src-dependent sites pY861 or pY925. Furthermore, our results show that p130Cas is likely a target of Src, and not FAK, in thyroid cancer cells, consistent with recent studies in breast cancer using a structurally distinct FAK kinase inhibitor, PND-1186 (27).

Finally, we evaluated the regulation of ERK and Akt signaling in response to FAK kinase inhibition, given the important role of these oncogenic pathways in thyroid cancer. In addition, both the BCPAP and 8505C cells express the BRAF V600E mutation. Figure 1A shows that FAK kinase inhibition does not affect phospho-ERK1/2 levels, consistent with mutant-BRAF driving ERK activity in these cells. Interestingly, phosphorylation of Akt (at S473) was decreased in response to FAK inhibition (Figure 1A) indicating FAK may rely on Akt for signaling responses.

To begin to define the role of FAK kinase activity in tumorigenic processes, the effects of FAK kinase inhibition on adherent growth was evaluated by cell viability assays. We observed that FAK kinase activity is dispensable for adherent cell growth in both the BCPAP and 8505C cells, as treatment with 1μM PF-573,228 did not significantly inhibit cell growth (Figure 1B). These results are consistent with other tumor models, where FAK kinase activity has modest effects on adherent cell growth (27,28). In addition, no enhanced sensitivity to FAK inhibition was observed in the presence of fibronectin, suggesting that integrin activation does not alter dependency on FAK activity in thyroid cancer cell lines (Figure S1). Of note, dual inhibition of FAK and PYK2 by treatment with PF-562,271 (Pfizer), also had minimal effects on adherent growth of thyroid cancer cells *in vitro* (data not shown), suggesting that compensatory PYK2 signaling is not important. We next evaluated the role of FAK on anchorage-independent growth, where FAK scaffolding and kinase activity have been shown to play an important role in other tumor types, including ovarian and breast cancer (29–31). We performed colony formation assays where the BCPAP and 8505C cells were exposed to 1 μM PF-573,228 for 20 days. While FAK kinase inhibition did not affect adherent cell growth (Figure 1B), Figure 1C shows that FAK kinase inhibition with PF-573,228 effectively inhibited colony formation by ~60% in the BCPAP cells ($p \leq 0.05$, *t-test)*, but did not significantly affect colony formation in the 8505C cells (~20%: *p=n.s., t-test*). We also tested the effects of FAK kinase inhibition on additional thyroid cancer cell lines under adherent and anchorage independent conditions. Figure S2A shows that with the exception of the C643 and TPC1 cells, the majority of thyroid cancer cell lines tested are relatively resistant to FAK kinase inhibition under adherent conditions (IC50 > 1 μM). Enhanced sensitivity to PF-573,228 treatment under anchorage-independent conditions was also observed in the RAS-mutant C643 cells, while the remaining thyroid cancer cell lines exhibited similar sensitivities in adherent and anchorage-independent conditions (Figure S2A and S2B). Together these data indicate that for certain thyroid cancer cell lines, FAK activity is more important in a three-dimensional, anchorage-independent environment. However, the precise mechanisms mediating this response remain under investigation, but appear to be independent of oncogene mutation status.

To begin to define the role of both FAK scaffolding and kinase functions in thyroid tumorigenesis, a genetic approach was used to generate cells lacking FAK protein expression. Specifically, two independent shRNA constructs targeting FAK (shFAK-1 and shFAK-2) or a scrambled control were introduced into cells via lentiviral transduction. After short-term selection, Western blot analysis showed efficient knockdown of total FAK in both the BCPAP and 8505C cells, which corresponds to a loss of pY397FAK (Figure 2A). Similar to inhibition of FAK kinase activity (Figure 1A), pY416Src levels were not consistently decreased by expression of shFAK, indicating that Src phosphorylation is not dependent on FAK expression or activity (Figure 2A). In addition, pAkt levels were not consistently regulated by knockdown of FAK expression. Finally, phospho-ERK1/2 levels were not affected by knockdown of FAK expression, consistent with ERK being a target of oncogenic BRAF, but not FAK, in these cells (Figure 2A).

In order to define the role of FAK expression on adherent cell growth, growth of BCPAP and 8505C cells expressing shFAK or scrambled control was assessed by ViCell counting (Figure 2B). FAK knockdown resulted in ~50–65% growth inhibition in the BCPAP cells, and ~50% inhibition of 8505C cells (BCPAP shFAK1: $p \leq 0.01$, *shFAK2:* $p \leq 0.05$, *t-test*; 8505C shFAK1: $p \leq 0.01$, *t-test*; shFAK2: $p \leq 0.01$, *t-test*). Both FAK kinase activity and expression have been shown to promote anchorage independent growth in certain cellular contexts (32,33). As shown in Figure 2C, the BCPAP cells are extremely sensitive to the loss of FAK expression, with a reduction in colony formation of ~80–90% ($p \leq 0.0001$, *t-test*). Colony formation was also significantly decreased by ~60–80% in the 8505C cells with FAK protein knockdown (shFAK1: $p \leq 0.0001$; shFAK2: $p \leq 0.01$, t-test). Taken together with the inhibition of FAK kinase activity, these results indicate that both adherent and anchorage-independent growth of thyroid cancer cells is predominately regulated by FAK protein expression (Figure 1B, 1C, 2B, and 2C).

Tumor growth is differentially regulated by FAK kinase activity and expression

We next evaluated the role of FAK kinase activity versus expression in tumor establishment and growth using the orthotopic thyroid cancer model (9,34–38). To assess the role of FAK kinase activity, BCPAP or 8505C cells engineered to stably express a luciferase-IRES-GFP plasmid were injected into the right thyroid gland of athymic nude mice, as previously described (9). Tumor establishment and progression was monitored by detection of bioluminescence. Mice were randomized after tumor establishment on day 10 and treated daily with the orally available and structurally related FAK/PYK2 kinase inhibitor PF-562,271 (50mg/kg) (32,39). Using this model, we observed significant inhibition of BCPAP orthotopic tumor growth after 14 days of FAK inhibitor treatment (day 24: $p \leq 0.01$, *t-test*), as compared to the vehicle-treated control mice (Figure3A and 3B). Overall, treatment with PF-562,271 resulted in ~40% reduction in BCPAP orthotopic final tumor volume, average of 125.58 ± 87.03 mm^3, while vehicle-treated control mice developed orthotopic tumors with an average volume of 213.34 ± 95.12 mm^3 ($p \leq 0.05$, *t-test*; Figure 3C). Finally, we observed a significant decrease in pY397FAK levels in FAK inhibitor-treated mice compared to vehicle-treated controls by immunohistochemical analysis (Figure3D and 3F, $p \leq 0.05$, *t-test*).

Similar to the BCPAP (PTC) tumors, we also observed a significant inhibition of tumor growth in the 8505C orthotopic model 14 days after treatment with PF-562,271 (day 24: $p \leq 0.05$, t-test) (Figure4A and 4B). While a significant difference in bioluminescence imaging was not observed at the final time point, average final tumor volumes for vehicle-treated mice versus PF-562,271 treated mice were 84.25 ± 19.22 mm^3 and 55.86 ± 35.03 mm^3, respectively, with a decrease in tumor growth of 34% ($p \leq 0.05$, t-test) (Figure 4C), indicating PF-562,271 treatment results in significant inhibition of tumor growth. We also observed that expression of pY397FAK was significantly decreased in the 8505C tumors treated with PF-562,271 compared to vehicle-treated controls (Figure4D and 4F: $p \leq 0.01$, *t-test*).

Due to the important role of FAK signaling in tumor invasion (21), we next evaluated whether inhibition of FAK kinase activity would disrupt this process. Interestingly, we did not observe a significant difference in invasion with FAK inhibitor treatment in the BCPAP or 8505C orthotopic models (Figure3E and 4E). Consistently, *in vitro* invasion assays using Matrigel-coated transwell chambers in the presence or absence of FAK kinase inhibitor (1 μM PF-573,228) was also not significantly inhibited (Figure S3A). We next evaluated the effects of FAK kinase inhibition on proliferation *in vivo*. Similar to the effects of FAK kinase inhibition on *in vitro* cell growth (Figure 1B), Ki67 staining of FAK inhibitor treated tumors did not reveal significant change in proliferation compared to vehicle tumors (Figure S4A and S4B). Additionally, FAK has been shown to play a key role in angiogenesis through its function in endothelial cells (40). However, CD34 staining, a marker of mouse endothelial cells, revealed no change in angiogenesis in the orthotopic tumors in response to FAK kinase inhibition (Figure S5A and S5B). Together, these data indicate that the kinase activity of FAK contributes to the pro-tumorigenic processes necessary for thyroid tumor progression, although the mechanism(s) remain unclear.

Given the key role for FAK expression in the regulation of both adherent and anchorage independent thyroid cancer cell growth (Figure 2B and 2C), we next evaluated the role of FAK expression in thyroid tumor establishment and progression *in vivo.* Specifically, BCPAP or 8505C cells expressing either shFAK or scrambled control were injected into the thyroid glands of nude mice orthotopically, as described above. Representative images of mice injected with BCPAP cells expressing scrambled control or shFAK are shown in Figure 5B. Notably, tumor establishment was inhibited in the BCPAP shFAK group by bioluminescence (Figure5A and 5B), and no tumors were present at the time of dissection (Figure 5C). We observed a robust inhibition of 8505C tumor growth with shRNA knockdown of FAK, but in contrast to the BCPAP-derived tumors, the 8505C-derived tumors expressing shFAK were able to establish (Figure5D and 5E) and grow to an average final tumor volume of 19.98 ± 9.89 mm^3, representing an ~80% average reduction in tumor volume compared to the scrambled control tumors ($p \leq 0.0001$, *t-test*; scrambled average final tumor volume of 122.5 +/− 45.67 mm^3; Figures 5F). In contrast to FAK kinase inhibition (Figures 3E and 4E), we observed that FAK knockdown significantly inhibited invasion in the 8505C orthotopic model (Figure5G and 5H, $p \leq 0.01$, *t-test*), despite having no effect on invasion *in vitro* (Figure S3B). However, in contrast to our *in vitro* data (Figure 2B), FAK depletion did not significantly affect cellular proliferation *in vivo*, as measured by Ki67 staining (Figure S6). Taken together, these data indicate that FAK expression plays a key

role in tumor establishment and/or progression, as well as invasion, of thyroid cancer cells *in vivo* and that FAK kinase activity may be more important for tumor progression.

Inhibition of FAK kinase activity reduces PTC metastasis *in vivo* but increases metastasis in an ATC model

FAK has been shown to play an important role in metastasis (31,41–43), but how FAK contributes to metastatic process, and whether pharmacological inhibition of FAK kinase activity will prevent or inhibit the development of metastases is not clear. In order to study the role of FAK in the development of distant metastases, we employed an intracardiac injection experimental metastasis model, which models the late stages of metastasis, including intravasation and organ colonization, and allows for the analysis of systemic tumor formation. We first asked whether FAK kinase inhibition would prevent the development of systemic tumor formation using a pretreatment approach, where mice were dosed with PF-562,271(50mg/kg) daily by oral gavage, two days before tumor cell injection, and treatment was continued throughout the experiment. The one-minute images shown in Figure 6B validate successful left ventricle injection and bioluminescent cell dissemination throughout the body. Weekly bioluminescence imaging of the BCPAP tumors shows that tumors treated with PF-562,271 exhibited a ~2-fold reduction in overall tumor burden compared to the vehicle treated counterparts ($p \leq 0.0001$, ANOVA; Figure6A and 6B), indicating that this pretreatment treatment approach has the potential to delay metastatic progression in this model.

To determine the role of FAK kinase activity in ATC metastasis, 8505C cells expressing luciferase were evaluated using the same pretreatment treatment approach described in Figure 6, where mice were treated with PF-562,271 two days before tumor cell injection, and treatment was continued throughout the experiment. Successful left ventricle injection of 8505C cells is shown in Figure 7C (1 minute images). Surprisingly, weekly imaging revealed a significant 1.5-fold increase in total tumor burden with this FAK inhibitor pretreatment approach (day 7: $p \leq 0.01$, day 14: $p \leq 0.05$, day 21: $p \leq 0.05$, day 35: $p \leq 0.001$; *t-test*; Figure7A and 7C). The increase in 8505C tumor formation using the pretreatment approach was observed in two different experiments, and this data is combined in Figure 7A. Due to the unexpected increase in tumor burden in response to PF-562,271 pretreatment, we asked if this was due to the timing of PF-562,271 treatment. Therefore, we used a post-treatment approach, where PF-562,271 (50mg/kg) was administered 8 days after intracardiac injection of the 8505C cells, when tumors have established. Interestingly, the post-treatment approach with PF-562,271 resulted in a 3.7-fold decrease in overall tumor burden ($p \leq 0.01$, *t-test*), with final tumor burden of $1.83 \times 10^9 \pm 1.04 \times 10^9$ photons/second for vehicle-treated mice and $4.98 \times 10^8 \pm 1.73 \times 10^8$ photons/second for the post-treatment group (Figure7B and 7C). Together, these results indicate that the response of the 8505C tumors is dependent on the timing of FAK inhibitor treatment, where the pretreatment approach increases overall tumor burden, and the post-treatment approach reduces overall tumor burden. Interestingly, analysis of *ex vivo* imaging shows an increase in metastasis to the bone of PF-562,271 pre-treated mice compared to either vehicle-treated or PF-562,271 post-treated mice (Figure S7), suggesting that the mechanism(s) of this response may be specific to the bone.

FAK expression regulates thyroid cancer metastasis

To determine the role of FAK expression in metastasis, cells expressing shFAK and a scrambled control shRNA were tested in the experimental metastasis model, as described above (Figures 6 and 7). Because FAK expression abolished tumor establishment in an orthotopic model of PTC (Figure 5A–C), the experimental metastasis model was employed only in the 8505C (ATC) cells. Consistent with the role of FAK expression in adherent and anchorage independent growth (Figure 2B–C), as well as orthotopic tumor growth (Figure 5A–F), overall tumor formation was significantly inhibited (20.6-fold reduction) in mice injected with 8505C shFAK expressing cells as compared to cells expressing scrambled shRNA (Figure 8A–B; $p \leq 0.001$; *ANOVA*). These results indicate that FAK expression plays a key role in the development and/or progression of metastases.

DISCUSSION

There are currently limited effective therapies for patients with advanced thyroid cancer, especially those with distant metastases (4). We have previously shown that FAK is overexpressed and activated in thyroid tumors, as well as in cell lines derived from advanced thyroid cancer patients (8). However, it is unclear how the functions of FAK mediate thyroid cancer, and whether the kinase or scaffolding functions of FAK are more important. Inhibitors targeting the kinase activity of FAK have provided an opportunity to directly test the role of FAK kinase activity and are currently being tested in clinical trials (18). Herein, we provide evidence that FAK expression versus kinase functions play distinct roles in thyroid cancer. Furthermore, we identify FAK expression as critical for thyroid cancer growth and metastasis, providing a new molecular target for advanced thyroid cancer.

In this study, we show that inhibition of FAK kinase activity with the selective small molecule inhibitor, PF-573,228, results in the inhibition of FAK Y397 autophosphorylation, without inhibition of p130Cas or Src phosphorylation. While these results are somewhat surprising, they are consistent with recent studies in breast cancer using the PND-1186 FAK kinase inhibitor (27). In addition, we did not observe regulation of ERK1/2 in response to inhibition of FAK kinase activity or expression (Figure1A and 2A), indicating that FAK does not regulate this oncogenic pathway in thyroid cancer. Consistent with this, we have not observed a correlation between sensitivity to FAK kinase inhibition and mutational status (BRAF, RAS, or RET/PTC; Figure S2 and data not shown). However, we did observe FAK-mediated regulation of Akt in response to FAK kinase inhibition (Figure 1A), although, changes in Akt did not correlate with response to growth inhibition (Figures 1B and 1C), indicating other mechanisms are involved. Thus, the precise pathways regulated by FAK in thyroid cancer are currently not clear, but likely involve noncanonical signaling pathways, including p38, as observed in breast cancer (39).

In addition to distinct signaling mechanisms, our results demonstrate that FAK kinase and expression regulate distinct processes in thyroid cancer, and FAK expression is the critical mediator of pro-tumorigenic processes. Specifically, adherent growth in both the BCPAP and 8505C cells was regulated predominantly by FAK expression, as FAK knockdown via shRNA displayed ~60–80% growth inhibition, while inhibition of kinase activity with PF-573,228 had minimal effects (Figure 2B and 1B). shRNA depletion of FAK resulted in a

significant loss of colony formation of both the BCPAP and 8505C cells (Figure 2C). Interestingly, while FAK kinase inhibition had limited effects under adherent conditions (Figure 1A and S2A), inhibition of kinase activity decreased colony formation by 20–80% (Figure 1C and S2B). These results are consistent with other tumor types, where inhibition of FAK kinase activity has had limited effects on proliferation under adherent growth conditions, but more striking affects under nonadherent conditions (27). The modest effects of FAK kinase inhibition are likely not due to compensatory upregulation of the related PYK2, as we did not observe an increase in total or phosphorylated PYK2 levels in response to FAK kinase inhibition (data not shown). Due to the lack of Src inhibition in response to FAK kinase inhibition (Figure 1A), we also asked whether inhibition of Src in combination with FAK kinase inhibition was necessary to achieve inhibition of adherent growth. However, combined FAK and Src inhibition did not enhance growth inhibition compared to Src inhibition alone (data not shown).

The results of our *in vivo* studies are consistent with our *in vitro* data, and show modest, but significant, effects of FAK kinase inhibition with PF-562,271 on thyroid tumor progression (Figure 3 and 4). These *in vivo* results are also consistent with studies in other tumor types, including breast, pancreas, and prostate cancer, where inhibition of FAK kinase activity results in modest inhibition of tumor development (27,32,41). In these models, the effects of FAK kinase inhibition have been attributed to attenuated survival signaling (through AKT), increased apoptosis, and altered expression of cytokines such as IL-6, which may impact tumor progression through effects on both tumor and stromal cells (27,41,44). In contrast to FAK kinase inhibition, FAK knockdown completely blocked tumor establishment/progression in the BCPAP orthotopic model (Figure 5A–C), and robustly inhibited tumor progression in the 8505C orthotopic model (Figure 5D–F). Similar results were observed in the metastatic model, suggesting that FAK expression is critical for tumor establishment and/or progression (Figure 8). Genetic studies targeting FAK have also revealed an important role for FAK in apoptosis, and that FAK is necessary for extravasation (16). While the precise mechanisms regulating tumor growth and establishment in response to FAK inhibition in thyroid cancer are not clear, inhibition of FAK kinase activity or expression does not affect cancer cell proliferation or microvessel density (Figure S4 and S5). Future studies will be needed to evaluate anti-tumor responses at earlier time points to assess the contribution of apoptosis and other processes that may affect tumor establishment, such as cytokine expression and Akt signaling.

In our metastasis studies, paradoxically, we found that pretreatment of mice with the PF-562,271 FAK kinase inhibitor enhanced systemic tumor formation in the 8505C model, while a post-treatment approach decreased tumor burden (Figure 7). These data indicate that while inhibition of FAK kinase activity can exhibit anti-tumor and anti-metastatic activity, under certain treatment conditions, may promote tumor formation. Along these lines, recent evidence suggests a non-linear function of FAK expression where homozygous depletion of endothelial FAK inhibits angiogenesis and decreases final tumor volume, while FAK-heterozygous mice have enhanced tumor angiogenesis and increased tumor volumes (44). This phenotype was associated with increased Akt and MAPK signaling, providing a potential mechanism for enhanced cell survival and migration. Interestingly, the results obtained from the FAK-heterozygous mice were phenocopied using FAK kinase inhibitors

(44). In addition, other studies have shown that FAK kinase activity negatively regulates invadopodia activity, thus inhibition of FAK can actually increase invasion (45,46). Given this complicated role of FAK, it remains possible that inhibition of FAK kinase activity may provide an advantage for cancer cell survival and invasion, resulting in enhanced metastasis, as observed here.

Interestingly, ex vivo imaging of vehicle, pre-treated, and post-treated mice revealed that mice pre-treated with PF-562,271 had a higher incidence of metastases to the bone compared to either of the other groups. Intriguingly, a growing group of literature suggests a role for FAK phosphorylation and expresion in the regulation of bone resorption, and *in vivo* studies of other cancer types indicate that the rate of bone turnover enhances the occurrence and progression of metastasis to the bone (47–50). In addition, bone resportion has been linked to enhanced metastatic growth in other tumor types including breast and prostate (49,51). Furthermore, other studies have suggested that the interaction between bone cells and cancer cells is critical in governing colonization of the bone (52). Although more studies are needed, these findings point to a potential mechanism mediating an enhanced metastatic phenotype, likely through the affect of FAK inhibition on bone cells and bone resportion.

Finally, the scaffolding role of FAK provides binding sites for multiple oncogenic tyrosine kinases including EGFR, c-MET, and Src, as well as tumor suppressors protein such as p53 and NF-1 (53). Therefore, the FAK scaffold provides a pool of potential targets, each of which controls highly specific aspects of kinase/signaling pathways. Numerous studies have demonstrated that FAK scaffolding is important in the development, maintenance, and dissemination of cancer (54–57). Thus, ongoing studies are currently dedicated to identifying specific effector proteins and signaling pathway(s) mediated by FAK scaffolding functions, which will ultimately allow us to target key protein-protein interactions to inhibit FAK-mediated pro-tumorigenic processes important for thyroid cancer establishment and metastasis, and further dissect the role of FAK kinase activity in these processes.

In conclusion, we have shown that inhibition of FAK expression versus kinase activity regulates distinct pro-tumorigenic processes, and importantly, that FAK expression is critical for the regulation of key thyroid tumorigenic functions, including anchorage-independent growth, tumor establishment/progression, and systemic tumor formation. Furthermore, knockdown of FAK was able to inhibit growth and tumor establishment in BRAF-mutant thyroid cancer models, independent of ERK1/2 signaling, demonstrating that these cells are also dependent on FAK signaling for growth and survival, and provides strong preclinical rationale for targeting FAK in the clinic. Finally, given that FAK functions in parallel to classical oncogenic signaling pathways in thyroid cancer, targeting these pathways in combination with FAK may reveal enhanced therapeutic efficacy in thyroid cancer.

Supplementary Material

Refer to Web version on PubMed Central for supplementary material.

Acknowledgments

We would like to thank Dr. Christopher Korch, UCCC, Department of Pathology, and Randall Wong at the B. Davis Center BioResources Core Facility, Molecular Biology Unit, for STR profiling of the cell lines. We also thank Drs. Arthur Gutierrez-Hartmann and Bryan Haugen for critical review of our manuscript. We also thank Pfizer for generously providing PF-573,228 and PF-562,271 for these studies.

GRANT SUPPORT:

This work was supported by NCI grant K12-CA086913 and NIH/NCI grant 1RO1CA164193-01A1 (RE Schweppe), and a UCCC Support Grant from the NCI (P30CA046934). The UCCC DNA Sequencing, UCD Research Histology Shared Resource and Small Animal Imaging Cores are supported by NCI Cancer Center, P30CA046934. The contents of this study are solely the responsibility of the authors and do not necessarily represent the official views of the NIH.

REFERENCES

1. Cancer of the Thyroid - SEER Stat Fact Sheets [Internet]. Available from: http://seer.cancer.gov/statfacts/html/thyro.html
2. Bernet V, Smallridge R. New therapeutic options for advanced forms of thyroid cancer. Expert Opin Emerg Drugs. 2014; 19:225–241. [PubMed: 24588376]
3. Gild ML, Bullock M, Robinson BG, Clifton-Bligh R. Multikinase inhibitors: a new option for the treatment of thyroid cancer. Nat Rev Endocrinol. 2011; 7:617–624. [PubMed: 21862995]
4. Pfister DG, Fagin JA. Refractory thyroid cancer: a paradigm shift in treatment is not far off. J Clin Oncol. 2008; 26:4701–4704. [PubMed: 18541893]
5. Irby RB, Yeatman TJ. Role of Src expression and activation in human cancer. Oncogene. 2000; 19:5636–5642. [PubMed: 11114744]
6. Kopetz S, Shah AN, Gallick GE. Src continues aging: current and future clinical directions. Clin Cancer Res. 2007; 13:7232–7236. [PubMed: 18094400]
7. Bolós V, Gasent JM, López-Tarruella S, Grande E. The dual kinase complex FAK-Src as a promising therapeutic target in cancer. Onco Targets Ther. 2010; 3:83–97. [PubMed: 20616959]
8. Schweppe RE, Kerege AA, French JD, Sharma V, Grzywa RL, Haugen BR. Inhibition of Src with AZD0530 reveals the Src-Focal Adhesion kinase complex as a novel therapeutic target in papillary and anaplastic thyroid cancer. J Clin Endocrinol Metab. 2009; 94:2199–2203. [PubMed: 19293266]
9. Chan CM, Jing X, Pike LA, Zhou Q, Lim D-J, Sams SB, et al. Targeted inhibition of Src kinase with dasatinib blocks thyroid cancer growth and metastasis. Clin Cancer Res. 2012; 18:3580–3591. [PubMed: 22586301]
10. Golubovskaya VM, Kweh FA, Cance WG. Focal adhesion kinase and cancer. Histol Histopathol. 2009; 24:503–510. [PubMed: 19224453]
11. Kim SJ, Park JW, Yoon JS, Mok JO, Kim YJ, Park HK, et al. Increased expression of focal adhesion kinase in thyroid cancer: immunohistochemical study. J Korean Med Sci. 2004; 19:710–715. [PubMed: 15483349]
12. Owens LV, Xu L, Dent GA, Yang X, Sturge GC, Craven RJ, et al. Focal adhesion kinase as a marker of invasive potential in differentiated human thyroid cancer. Ann Surg Oncol. 1996; 3:100–105. [PubMed: 8770310]
13. Michailidi C, Giaginis C, Stolakis V, Alexandrou P, Klijanienko J, Delladetsima I, et al. Evaluation of FAK and Src expression in human benign and malignant thyroid lesions. Pathol. Oncol. Res. 2010:497–507. [PubMed: 20405349]
14. Provenzano PP, Keely PJ. The role of focal adhesion kinase in tumor initiation and progression. Cell Adh Migr. 2009; 3:347–350. [PubMed: 19690467]
15. Siesser PMF, Hanks SK. The signaling and biological implications of FAK overexpression in cancer. Clin Cancer Res. 2006; 12:3233–3237. [PubMed: 16740741]
16. Pylayeva Y, Gillen KM, Gerald W, Beggs HE, Reichardt LF, Giancotti FG. Ras- and PI3K-dependent breast tumorigenesis in mice and humans requires focal adhesion kinase signaling. J Clin Invest. 2009; 119:252–266. [PubMed: 19147981]

17. Kurenova E, Ucar D, Liao J, Yemma M, Gogate P, Bshara W, et al. A FAK scaffold inhibitor disrupts FAK and VEGFR-3 signaling and blocks melanoma growth by targeting both tumor and endothelial cells. Cell Cycle. 2014; 13:2542–2553. [PubMed: 25486195]
18. Infante JR, Camidge DR, Mileshkin LR, Chen EX, Hicks RJ, Rischin D, et al. Safety, Pharmacokinetic, and Pharmacodynamic Phase I Dose-Escalation Trial of PF-00562271, an Inhibitor of Focal Adhesion Kinase, in Advanced Solid Tumors. J Clin Oncol. 2012; 30:1527–1533. [PubMed: 22454420]
19. Golubovskaya V. Targeting FAK in human cancer: from finding to first clinical trials. Front Biosci. 2014; 19:687–706.
20. Sulzmaier FJ, Jean C, Schlaepfer DD. FAK in cancer: mechanistic findings and clinical applications. Nat Rev Cancer. 2014; 14:598–610. [PubMed: 25098269]
21. Zhao J, Guan J. Signal transduction by focal adhesion kinase in cancer. Cancer Metastasis Rev. 2009; 28:35–49. [PubMed: 19169797]
22. Wood WM, Sharma V, Bauerle KT, Pike LA, Zhou Q, Fretwell DL, et al. PPARγ Promotes Growth and Invasion of Thyroid Cancer Cells. PPAR Res. 2011; 2011:171765. [PubMed: 22194735]
23. Chen XL, Nam J-O, Jean C, Lawson C, Walsh CT, Goka E, et al. VEGF-induced vascular permeability is mediated by FAK. Dev Cell. 2012; 22:146–157. [PubMed: 22264731]
24. Sieg DJ, Hauck CR, Ilic D, Klingbeil CK, Schaefer E, Damsky CH, et al. FAK integrates growth-factor and integrin signals to promote cell migration. Nat Cell Biol. 2000; 2:249–256. [PubMed: 10806474]
25. Hauck CR, Hsia DA, Schlaepfer DD. Focal adhesion kinase facilitates platelet-derived growth factor-BB-stimulated ERK2 activation required for chemotaxis migration of vascular smooth muscle cells. J Biol Chem. 2000; 275:41092–41099. [PubMed: 10998418]
26. Schlaepfer DD, Hunter T. Focal adhesion kinase overexpression enhances ras-dependent integrin signaling to ERK2/mitogen-activated protein kinase through interactions with and activation of c-Src. J Biol Chem. 1997; 272:13189–13195. [PubMed: 9148935]
27. Walsh C, Tanjoni I, Uryu S, Tomar A, Nam J-O, Luo H, et al. Oral delivery of PND-1186 FAK inhibitor decreases tumor growth and spontaneous breast to lung metastasis in pre-clinical models. Cancer Biol Ther. 2010; 9:778–790. [PubMed: 20234193]
28. Schultze A, Fiedler W, Prognostic I, Fak FAK. Therapeutic potential and limitations of new FAK inhibitors in the treatment of cancer. Expert Opin Investig Drugs. 2010; 19:777–788.
29. Tancioni I, Uryu S, Sulzmaier FJ, Shah NR, Lawson C, Miller NLG, et al. FAK Inhibition Disrupts a β5 Integrin Signaling Axis Controlling Anchorage-Independent Ovarian Carcinoma Growth. Mol Cancer Ther. 2014; 13:2050–2061. [PubMed: 24899686]
30. Xu LH, Yang X, Bradham CA, Brenner DA, Baldwin AS, Craven RJ, et al. The focal adhesion kinase suppresses transformation-associated, anchorage-independent apoptosis in human breast cancer cells. Involvement of death receptor-related signaling pathways. J Biol Chem. 2000; 275:30597–30604. [PubMed: 10899173]
31. Mitra S, Lim S-T, Chi A, Schlaepfer D. Intrinsic focal adhesion kinase activity controls orthotopic breast carcinoma metastasis via the regulation of urokinase plasminogen activator expression in a syngeneic. Oncogene. 2006; 25:4429–4440. [PubMed: 16547501]
32. Roberts WG, Ung E, Whalen P, Cooper B, Hulford C, Autry C, et al. Antitumor activity and pharmacology of a selective focal adhesion kinase inhibitor, PF-562,271. Cancer Res. 2008; 68:1935–1944. [PubMed: 18339875]
33. Hehlgans S, Lange I, Eke I, Cordes N. 3D cell cultures of human head and neck squamous cell carcinoma cells are radiosensitized by the focal adhesion kinase inhibitor TAE226. Radiother Oncol. 2009; 92:371–378. [PubMed: 19729215]
34. Ahn S-H, Henderson Y, Kang Y, Chattopadhyay C, Holton P, Wang M, et al. An orthotopic model of papillary thyroid carcinoma in athymic nude mice. Arch Otolaryngol Head Neck Surg. 2008; 134:190–197. [PubMed: 18283163]
35. Kim S, Park Y-W, Schiff BA, Doan DD, Yazici Y, Jasser SA, et al. An orthotopic model of anaplastic thyroid carcinoma in athymic nude mice. Clin Cancer Res. 2005; 11:1713–1721. [PubMed: 15755992]

36. Nucera C, Nehs MA, Mekel M, Zhang X, Hodin R, Lawler J, et al. A novel orthotopic mouse model of human anaplastic thyroid carcinoma. Thyroid. 2009; 19:1077–1084. [PubMed: 19772429]
37. Morrison JA, Pike LA, Sams SB, Sharma V, Zhou Q, Severson JJ, et al. Thioredoxin interacting protein (TXNIP) is a novel tumor suppressor in thyroid cancer. Mol Cancer. 2014; 13:62. [PubMed: 24645981]
38. Morrison JA, Pike LA, Lund G, Zhou Q, Kessler BE, Bauerle KT, et al. Characterization of thyroid cancer cell lines in murine orthotopic and intracardiac metastasis models. Horm Cancer. 2015; 6:87–99. [PubMed: 25800363]
39. Wendt MK, Schiemann WP. Therapeutic targeting of the focal adhesion complex prevents oncogenic TGF-beta signaling and metastasis. Breast Cancer Res. 2009; 11:R68. [PubMed: 19740433]
40. Lechertier T, Hodivala-Dilke K. Focal adhesion kinase and tumour angiogenesis. J Pathol. 2012; 226:404–412. [PubMed: 21984450]
41. Stokes JB, Adair SJ, Slack-Davis JK, Walters DM, Tilghman RW, Hershey ED, et al. Inhibition of focal adhesion kinase by PF-562,271 inhibits the growth and metastasis of pancreatic cancer concomitant with altering the tumor microenvironment. Mol Cancer Ther. 2011; 10:2135–2145. [PubMed: 21903606]
42. Provenzano PP, Inman DR, Eliceiri KW, Beggs HE, Keely PJ. Mammary epithelial-specific disruption of focal adhesion kinase retards tumor formation and metastasis in a transgenic mouse model of human breast cancer. Am J Pathol. 2008; 173:1551–1565. [PubMed: 18845837]
43. Miyazaki T, Kato H, Nakajima M, Sohda M, Fukai Y, Masuda N, et al. FAK overexpression is correlated with tumour invasiveness and lymph node metastasis in oesophageal squamous cell carcinoma. Br J Cancer. 2003; 89:140–145. [PubMed: 12838315]
44. Kostourou V, Lechertier T, Reynolds LE, Lees DM, Baker M, Jones DT, et al. FAK-heterozygous mice display enhanced tumour angiogenesis. Nat Commun. 2013; 4:2020. [PubMed: 23799510]
45. Kolli-Bouhafs K, Sick E, Noulet F, Gies J-P, De Mey J, Rondé P. FAK competes for Src to promote migration against invasion in melanoma cells. Cell Death Dis. 2014; 5:e1379. [PubMed: 25118939]
46. Chan KT, Cortesio CL, Huttenlocher A. FAK alters invadopodia and focal adhesion composition and dynamics to regulate breast cancer invasion. J Cell Biol. 2009; 185:357–370. [PubMed: 19364917]
47. Zhang Z, Neff L, Bothwell ALM, Baron R, Horne WC. Calcitonin induces dephosphorylation of Pyk2 and phosphorylation of focal adhesion kinase in osteoclasts. Bone. 2002; 31:359–365. [PubMed: 12231407]
48. Tanaka S, Takahashi N, Udagawa N, Murakami H, Nakamura I, Kurokawa T, et al. Possible involvement of focal adhesion kinase, p125FAK, in osteoclastic bone resorption. J Cell Biochem. 1995; 58:424–435. [PubMed: 7593264]
49. Buijs JT, Que I, Löwik CWGM, Papapoulos SE, van der Pluijm G. Inhibition of bone resorption and growth of breast cancer in the bone microenvironment. Bone. 2009; 44:380–386. [PubMed: 19041433]
50. Kostenuik PJ, Singh G, Suyama KL, Orr FW. Stimulation of bone resorption results in a selective increase in the growth rate of spontaneously metastatic Walker 256 cancer cells in bone. Clin Exp Metastasis. 1992; 10:411–418. [PubMed: 1451351]
51. Schneider A, Kalikin LM, Mattos AC, Keller ET, Allen MJ, Pienta KJ, et al. Bone turnover mediates preferential localization of prostate cancer in the skeleton. Endocrinology. 2005; 146:1727–1736. [PubMed: 15637291]
52. Bagi CM, Roberts GW, Andresen CJ. Dual focal adhesion kinase/Pyk2 inhibitor has positive effects on bone tumors: implications for bone metastases. Cancer. 2008; 112:2313–2321. [PubMed: 18348298]
53. Cance WG, Kurenova E, Marlowe TGV. Disrupting the Scaffold to Improve Focal Adhesion kinase-Targeted Cancer Therapeutics. Sci Signal. 2013; 6:pe10. [PubMed: 23532331]

54. Shen TL, Guan JL. Differential regulation of cell migration and cell cycle progression by FAK complexes with Src, PI3K, Grb7 and Grb2 in focal contacts. FEBS Lett. 2001; 499:176–181. [PubMed: 11418135]

55. Luo M, Fan H, Nagy T, Wei H, Wang C, Liu S, et al. Mammary epithelial-specific ablation of the focal adhesion kinase suppresses mammary tumorigenesis by affecting mammary cancer stem/progenitor cells. Cancer Res. 2009; 69:466–474. [PubMed: 19147559]

56. Luo M, Zhao X, Chen S, Liu S, Wicha M, Guan J. Distinct FAK activities determine progenitor and mammary stem cell characteristics. Cancer Res. 2013; 73:5591–5602. [PubMed: 23832665]

57. Sieg D, Hauck C, Ilic D, Klingbeil C. FAK integrates growth-factor and integrin signals to promote cell migration. Nat cell. 2000; 2:249–256.

Implications

This study demonstrates that FAK expression, but not kinase activity alone, predominantly mediates thyroid tumor growth and metastasis, indicating that targeting the scaffolding function(s) of FAK may be an important therapeutic strategy for advanced thyroid cancer, as well as other FAK-dependent tumors.

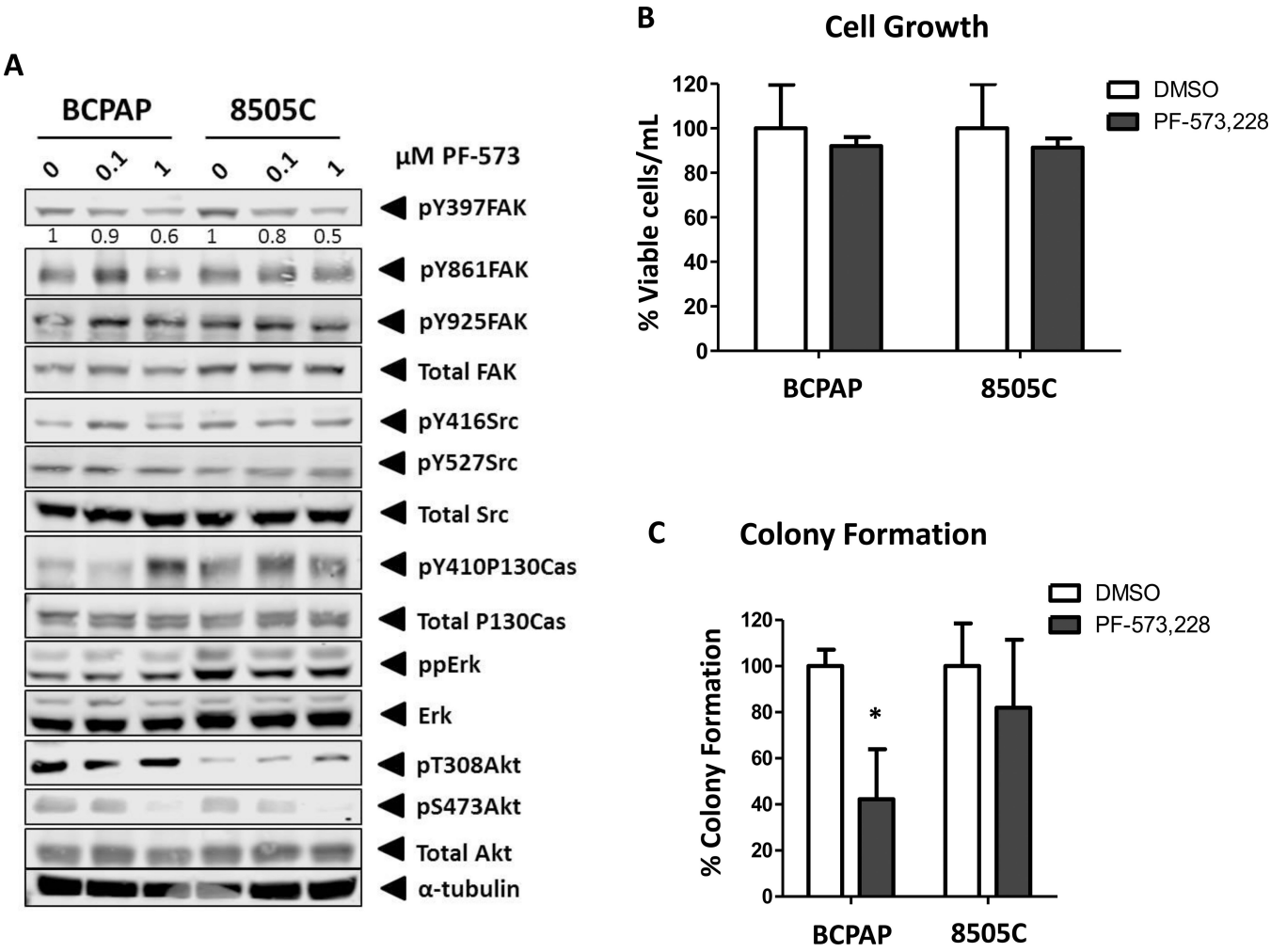

Figure 1. FAK kinase activity is dispensable for adherent growth but mediates anchorage-independent growth

(**A**) BCPAP and 8505C cells were treated with the indicated concentration of FAK inhibitor PF-573,228 for 24 hours. Blots shown are representative of 3 independent experiments. (**B**) Viability of BCPAP and 8505C cells treated with 1µM PF-573,228 for 6 days was normalized to DMSO-treated cells, set to 100%. Results are % viable cells per mL ± SD of 3 experiments performed in triplicate BCPAP PF-573: n.s; 8505C PF-573: n.s.). (**C**) Colonies of BCPAP and 8505C cells treated with 1µM PF-573,228 in soft agar were allowed to form for 20 days and normalized to DMSO-treated cells, set to 100%. Results shown are percent of colony formation ± SD of 3 independent experiments performed in duplicate (BCPAP PF-573: $p \leq 0.05$; 8505C PF-573: n.s).

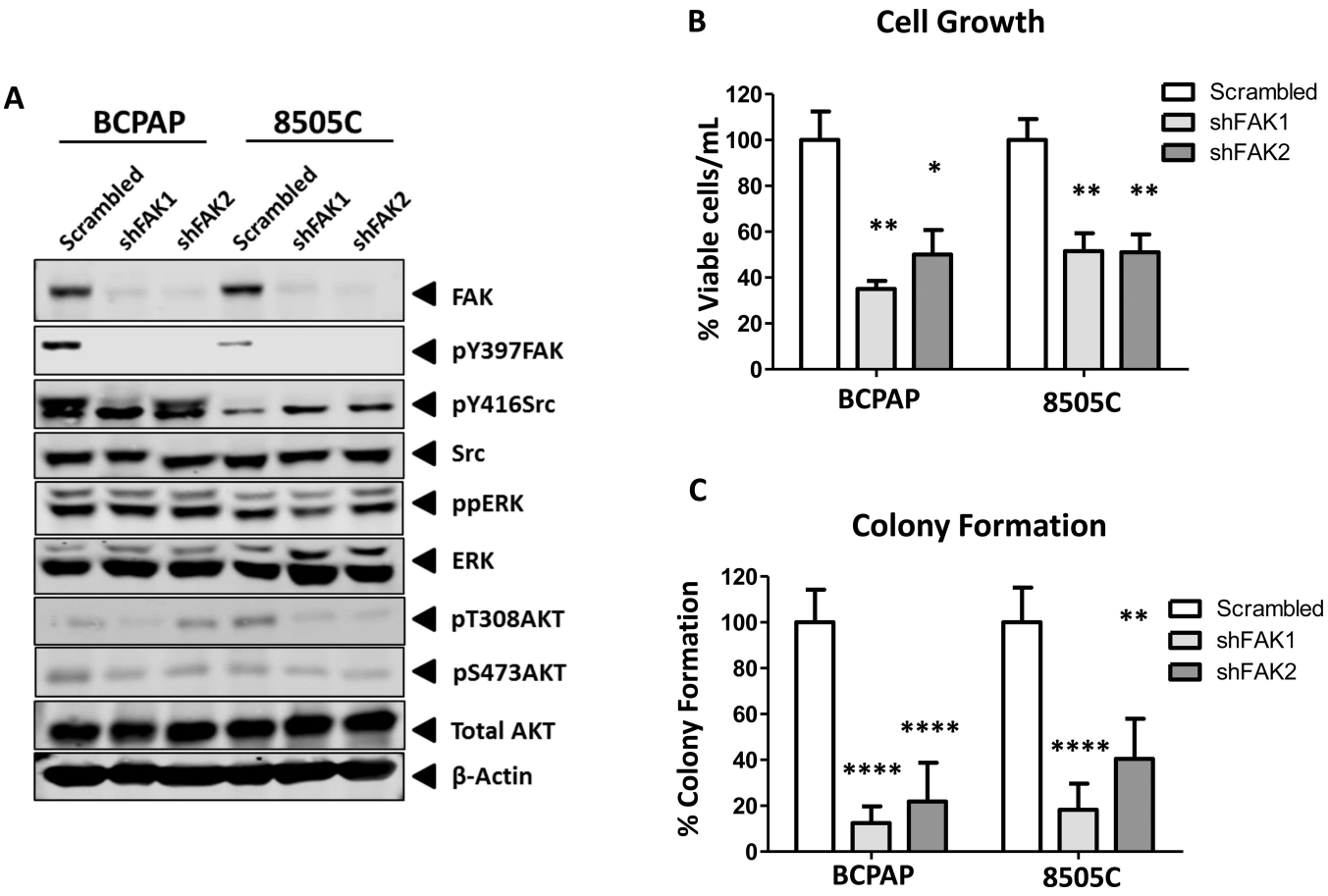

Figure 2. FAK expression mediates adherent and anchorage-independent growth

(**A**) BCPAP and 8505C cells expressing shRNA targeting FAK or a scrambled control were analyzed via Western blot. Blots are representative of 3 independent experiments (**B**) Viability of BCPAP and 8505C cells expressing shFAK was normalized to scrambled expressing cells, set to 100%. Results are % viable cells per mL ± SD of 3 experiments performed in triplicate (BCPAP shFAK1: $p \leq 0.01$ and shFAK2: $p \leq 0.05$; 8505C shFAK1 and shFAK2: $p \leq 0.01$). (**C**) Colonies of BCPAP and 8505C cells expressing shFAK were plated in soft agar, allowed to form colonies for 20 days and normalized to scramble cells, set to 100%. Results shown are percent of colony formation ± SD of 3 independent experiments performed in duplicate (BCPAP shFAK1 and shFAK2: $p \leq 0.0001$; 8505C shFAK1: $p \leq 0.0001$. shFAK2: $p \leq 0.01$).

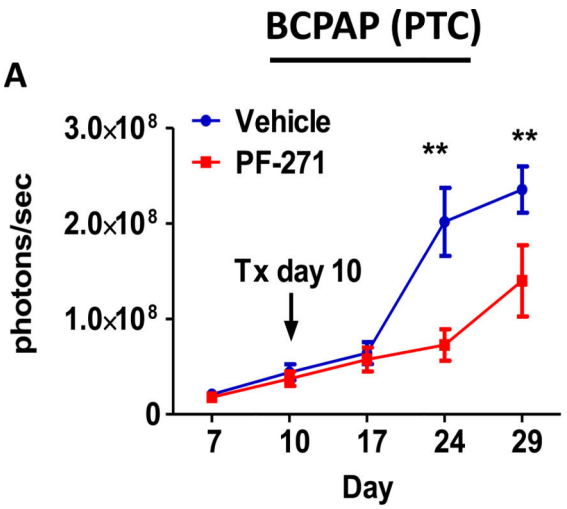

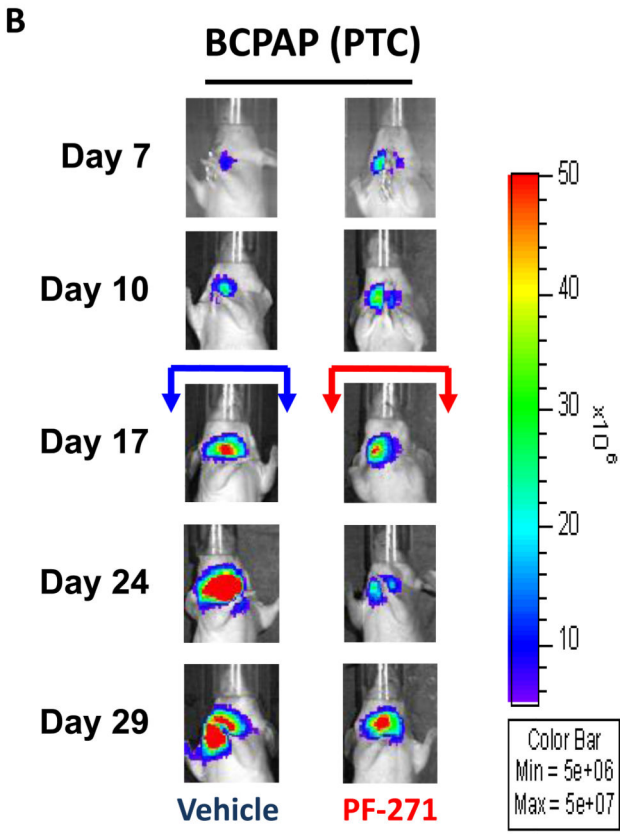

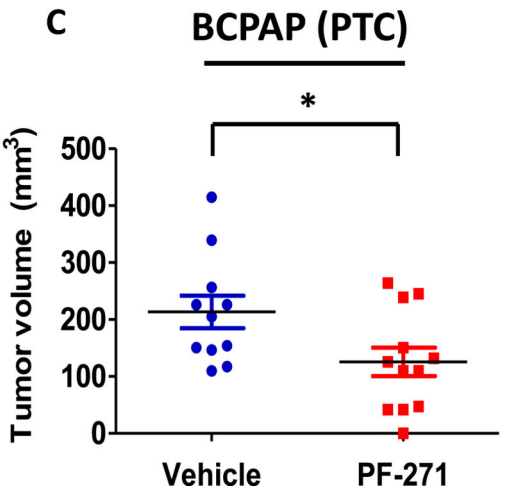

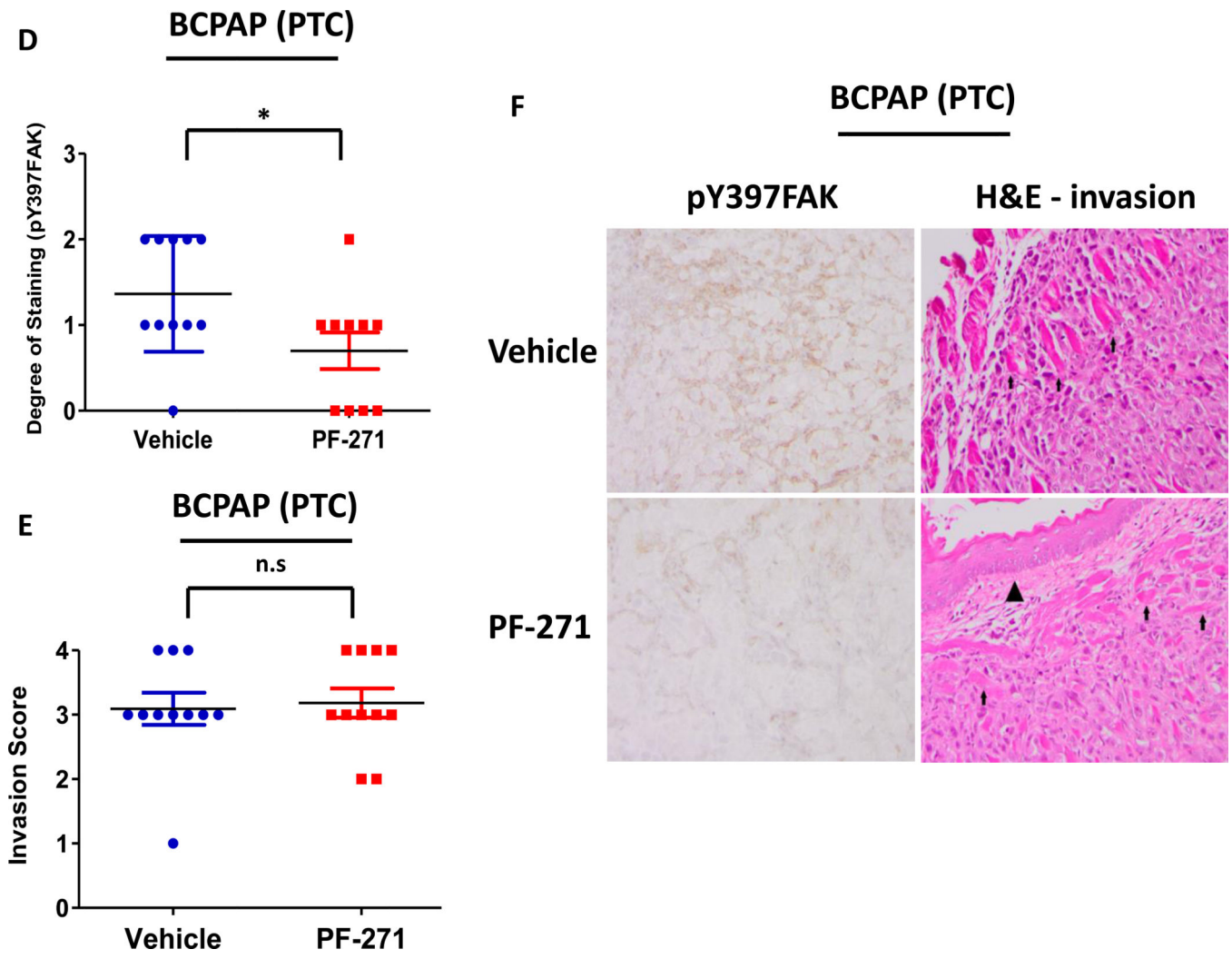

Figure 3. PTC orthotopic tumor growth is significantly reduced with FAK kinase inhibition

Mice were injected with BCPAP cells, randomized, and treated on day 10 with 50 mg/kg of PF-562,271 or vehicle for 29 days. (**A**) BCPAP tumor growth overtime was observed via bioluminescence signaling (day 24, $p \leq 0.01$; day 29 $p \leq 0.01$; *t-test*.). Results shown are mean bioluminescence signal (photons/second) per group ± SEM at the indicated time points. (**B**) Representative bioluminescence images for BCPAP are shown. (**C**) BCPAP tumors were collected at day 29 and size was measured with calipers. The final tumor volumes were calculated ($p \leq 0.05$, *t-test*). (**D**) IHC staining on BCPAP tumors was performed on sections of each tumor and scored as degree of staining by a pathologist. Results are degree of staining ± SEM ($p \leq 0.05$, t-test). (**E**) H&E staining was performed on BCPAP tumor sections and the percent of invasion was scored and calculated by a pathologist. Results are invasion scores ± SEM (p = n.s). (**F**) Representative images from IHC staining of pY397FAK (left) and H&E (right) or vehicle and PF-271 treated tumors are shown (200× magnification). H&E of vehicle-treated tumor shows invasion of poorly differentiated carcinoma into striated muscle Small arrows demonstrates muscle. H&E of PF-271-treated tumor shows invasion of poorly differentiated carcinoma into esophagus-adjacent muscle. Small arrows demonstrate muscle.

Arrowhead demonstrates esophageal squamous mucosa. (Hematoxylin-eosin, original magnification × 200).

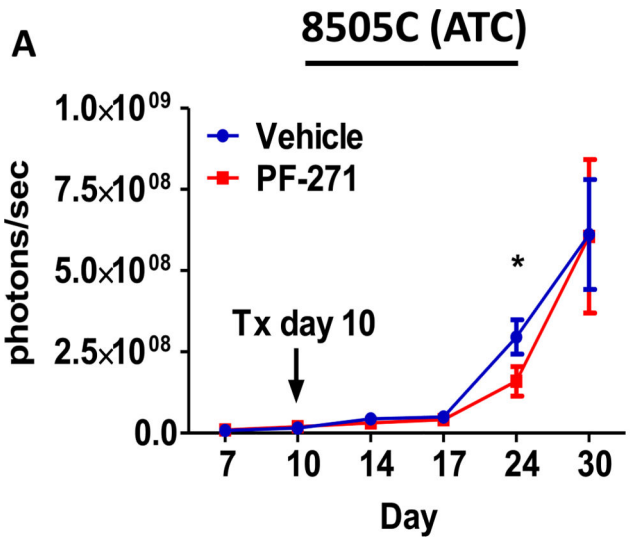

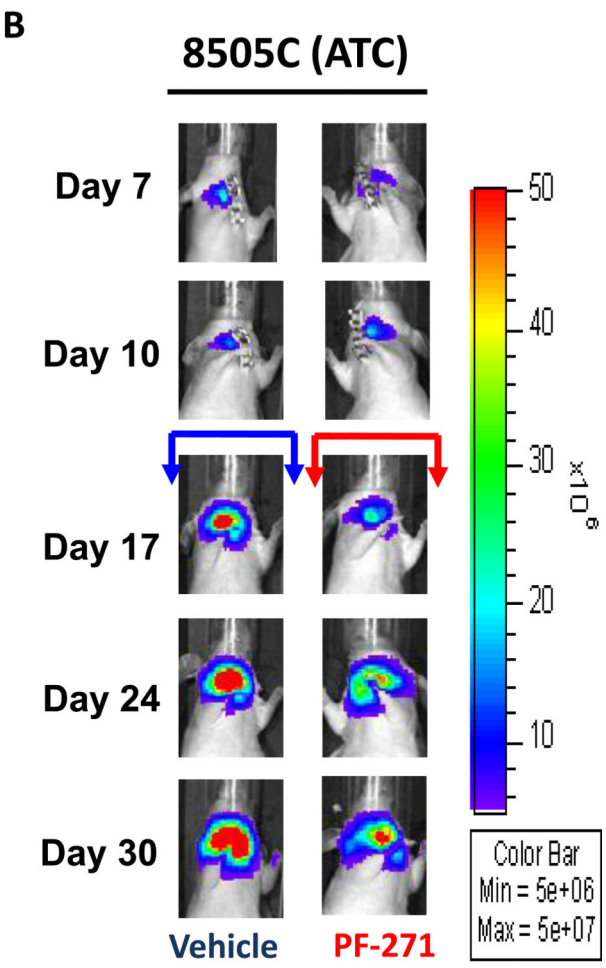

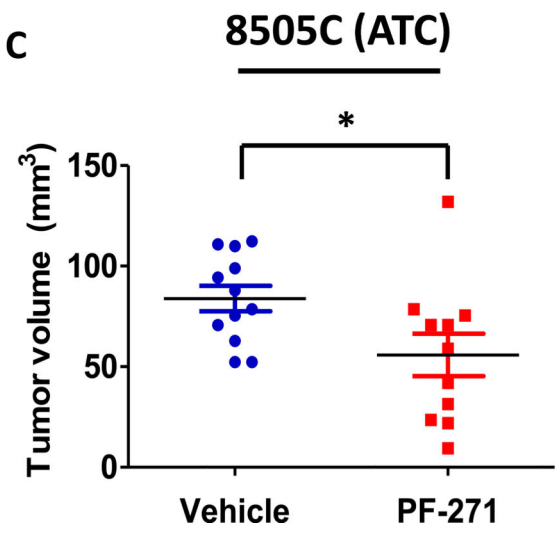

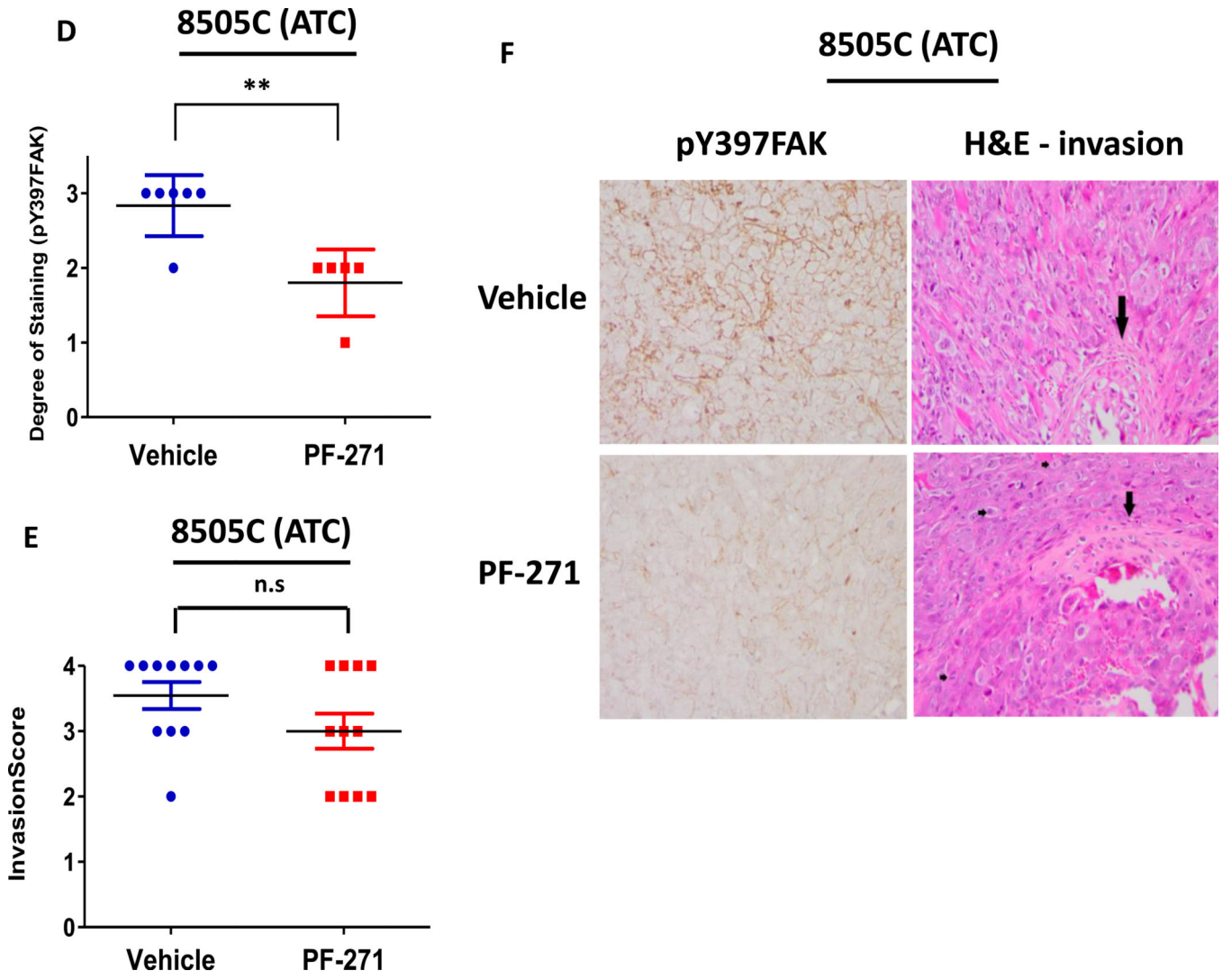

Figure 4. ATC orthotopic tumor growth is reduced with FAK kinase inhibition

Mice were injected with 8505C cells, randomized, and treated on day 10 with 50 mg/kg of PF-562,271 or vehicle for 30 days. (**A**) 8505C tumor growth overtime was observed via bioluminescence signaling (day 24, $p \leq 0.05$, *t-test*). Results shown are mean bioluminescence signal (photons/second) per group ± SEM at the indicated time points. (**B**) Representative bioluminescence images for 8505C are shown. (**C**) 8505C tumors were collected at day 30 and size was measured with calipers. The final tumor volumes were calculated ($p \leq 0.05$, *t-test*). (**D**) IHC staining on 8505C tumors was performed on sections of each tumor and scored as degree of positive staining by a pathologist. Results are degree of staining ± SD ($p \leq 0.01$, *t-test*). (**E**) H&E staining on 8505C tumors was performed on sections of each tumor. The percent of invasion was scored and calculated by a pathologist. Results are invasion scores ± SEM (p = n.s). (**F**) Representative images from IHC staining of pY397FAK (left) and H&E (right) of vehicle and PF-271 treated tumors are shown (200× magnification). H&E of vehicle-treated tumor shows invasion of poorly differentiated carcinoma through cartilage of trachea (large arrow). H&E of PF-271-treated tumor shows invasion of poorly differentiated carcinoma through cartilage of trachea (large arrow). Small

arrows demonstrate numerous mitotic figures. (Hematoxylin-eosin, original magnification × 200).

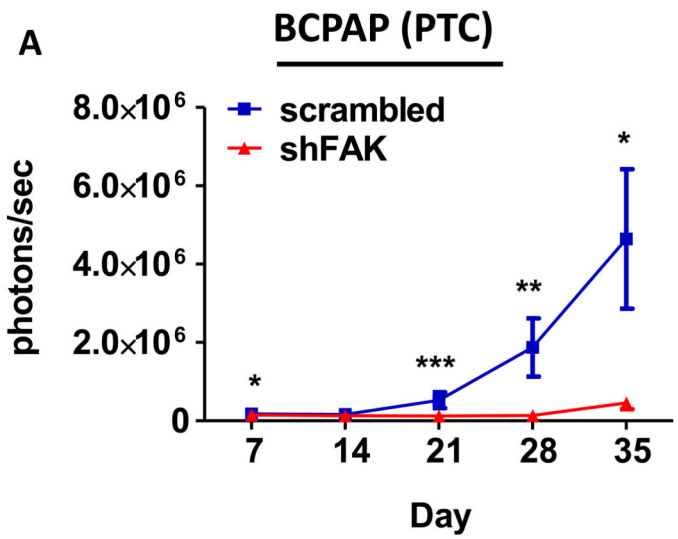

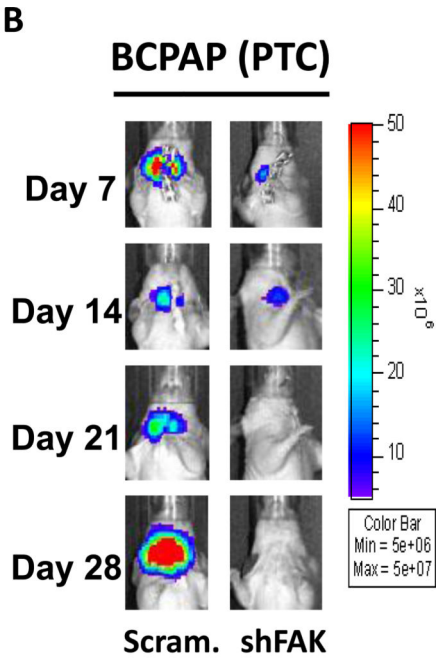

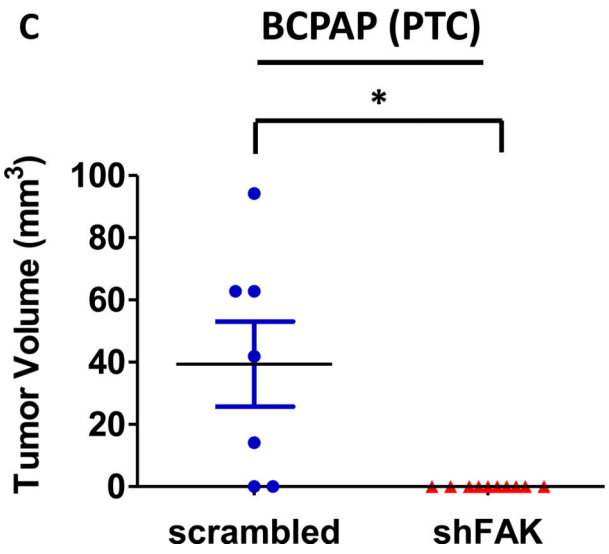

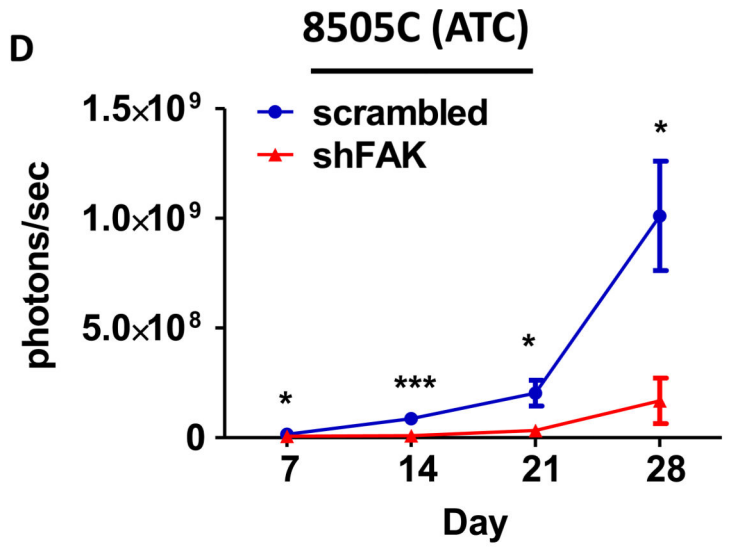

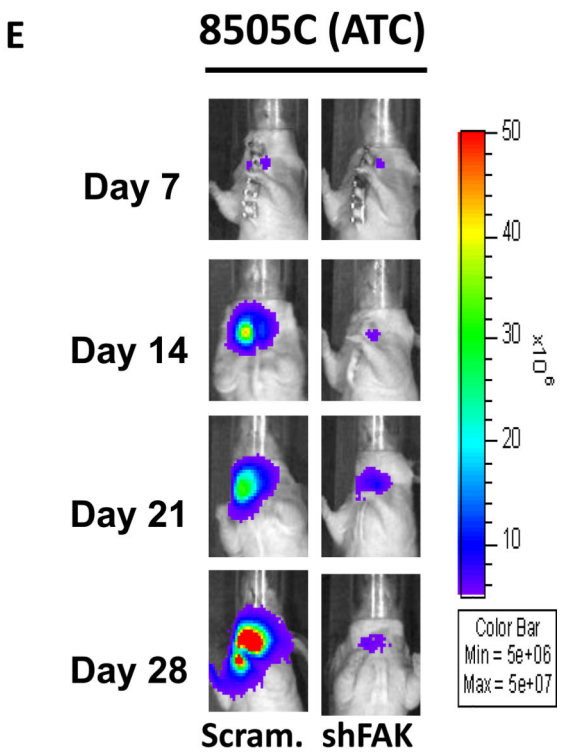

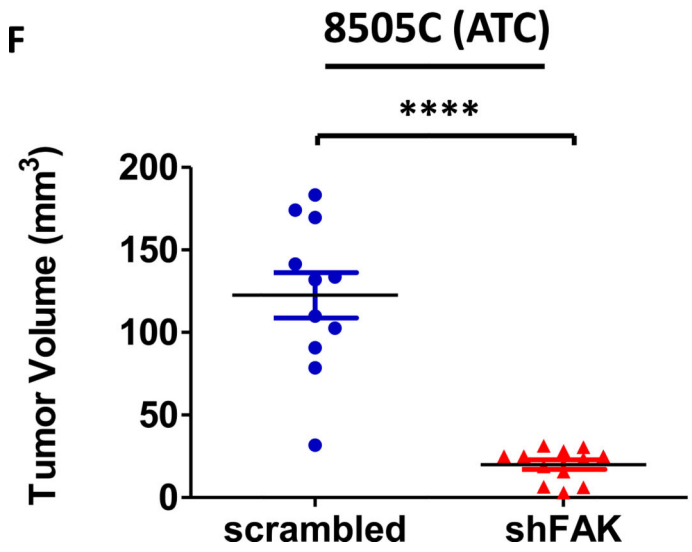

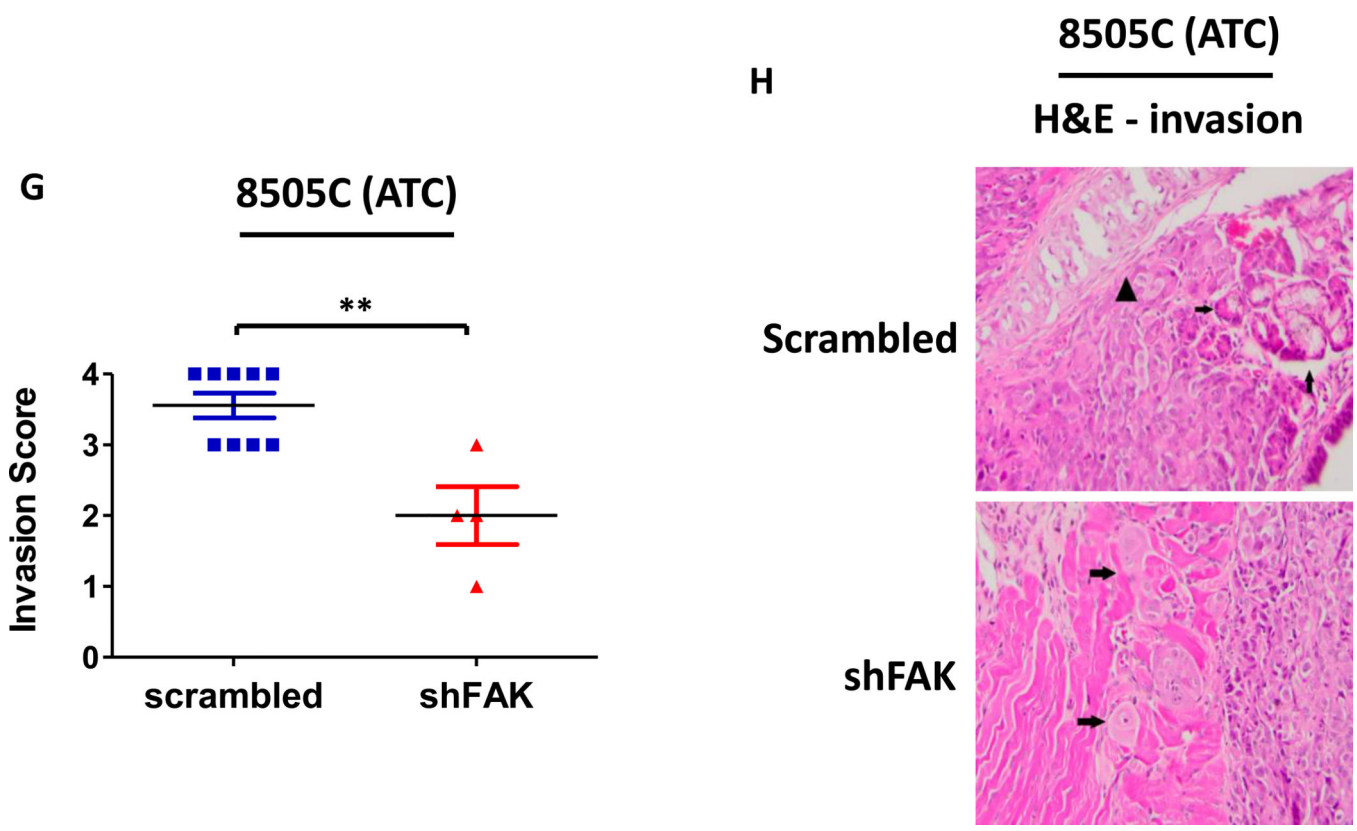

Figure 5. Loss of FAK expression significantly reduces tumor growth in ATC and prevents tumor establishment in PTC orthotopic models

Mice were injected with BCPAP or 8505C cells expressing either shFAK (shFAK1) or scrambled control shRNA. BCPAP (**A**) and 8505C (**D**) tumor growth was monitored overtime via bioluminescence imaging (BCPAP: day 7, $p \leq 0.05$; day 21, $p \leq 0.001$; day 28, $p \leq 0.01$; day 35, $p \leq 0.05$; *t-test*. 8505C: day 7, $p \leq 0.05$; day 14, $p \leq 0.001$; day 21, $p \leq 0.05$; day 28, $p \leq 0.01$; *t-test*). Results shown are mean bioluminescence signal (photons/second) per group ± SEM at the indicated time points. Representative bioluminescence images for BCPAP shFAK and scrambled tumors (**B**) and 8505C shFAK and scrambled tumors (**E**) are shown. Tumors were collected upon dissection (BCPAP = day 35; 8505C = day 28) and final tumor volumes for BCPAP (**C**) and 8505C (**F**) were calculated (BCPAP: $p \leq 0.05$; 8505C: $p \leq 0.0001$). (**G**) H&E staining was performed on sections of 8505C shFAK and scrambled orthotopic thyroid tumors. Invasion was scored and calculated by a pathologist. Results are invasion scores ± SEM ($p \leq 0.0001$, *t-test*). (**H**) Representative images are shown of H&E staining. H&E of scrambled-expressing tumor shows invasion of poorly differentiated carcinoma into trachea. Small arrows demonstrate salivary gland. Arrowhead demonstrates tracheal cartilage. (Bottom) H&E of shFAK-expressing tumor with arrows demonstrating invasion of tumor cells into adjacent muscle.

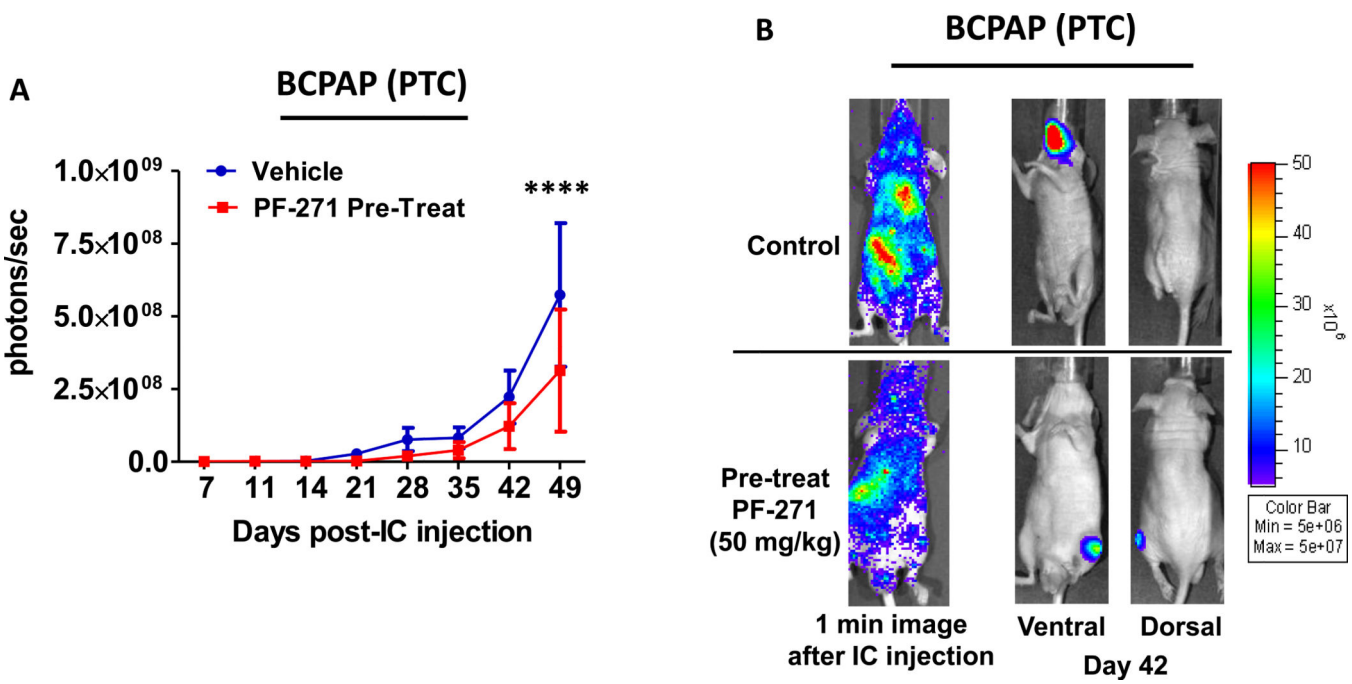

Figure 6. FAK kinase inhibition reduced PTC metastatic burden *in vivo*

Mice were pretreated with PF-562,271 (50mg/kg, 7d/w) 2 days prior to injection. Mice were injected with BCPAP cells. (**A**) Bioluminescence detection monitored metastatic progression over time (*p≤0.0001*; ANOVA). Results shown are mean bioluminescence signal (photons/second) per group ± SEM at the indicated time points. (Final total metastatic burden: Control = $5.74\times10^8 \pm 2.47\times10^8$ p/s; PF-271 treatment = $3.12\times10^8 \pm 2.10\times10^8$ p/s). (**B**) Representative bioluminescence images show 1 minute after injection to demonstrate dissemination. Ventral and dorsal images are shown for representative mice at day 42.

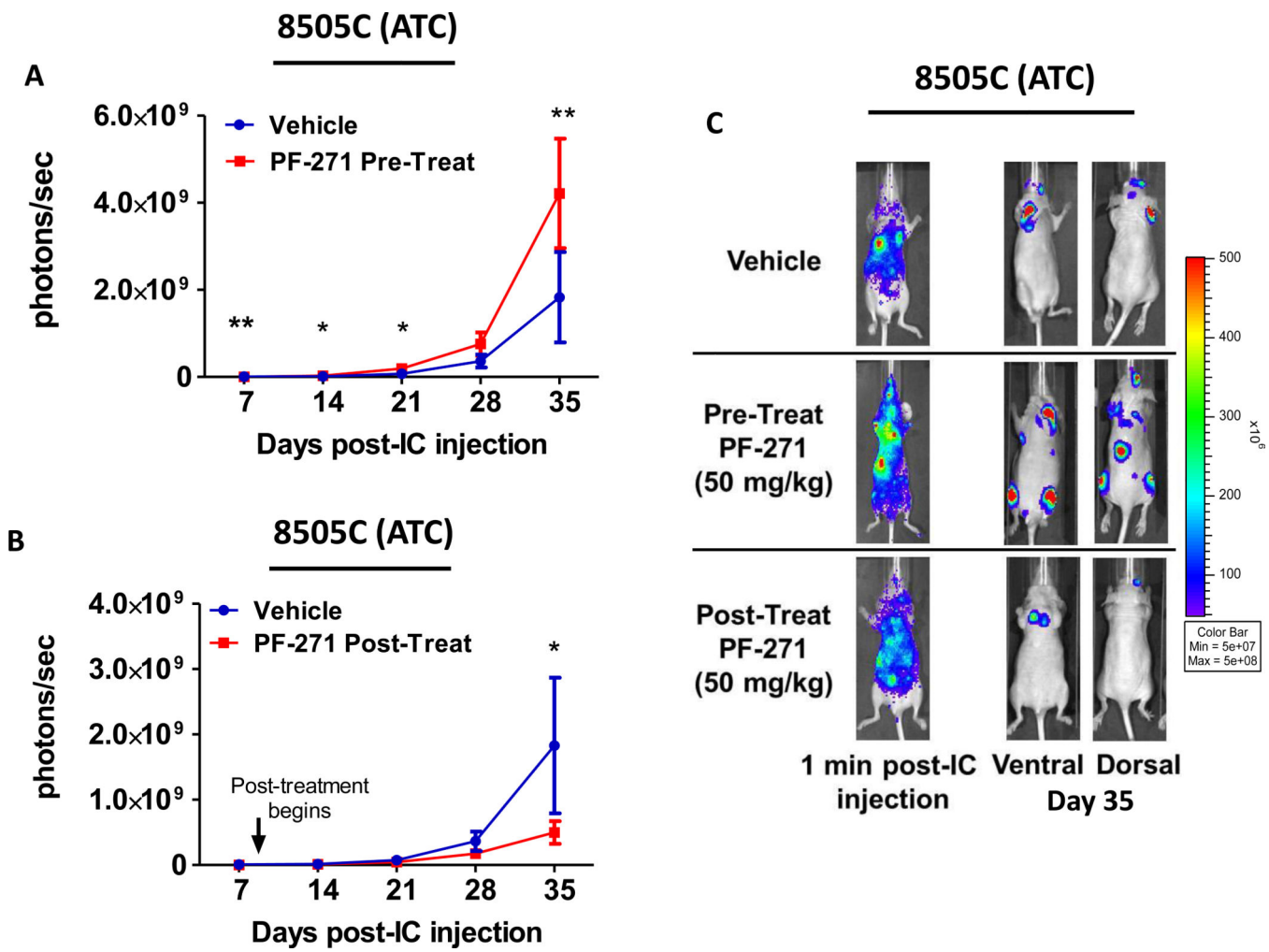

Figure 7. FAK kinase inhibition significantly enhances ATC metastasic burden *in vivo* using a pretreatment approach

Mice were injected with 8505C cells and either (**A**) pretreated with PF-562,271 (50mg/kg, 7d/w) 2 days prior to injection or (**B**) treated 8 days after injection (post-treat). Bioluminescence detection monitored metastatic progression over time (Pre-treatment: day 7, $p \leq 0.01$; day 14, $p \leq 0.05$; day 21, $p \leq 0.05$; day 35, $p \leq 0.001$; *t-test*. Post-treatment: day 35, $p \leq 0.01$; *t-test)*. Results shown are mean bioluminescence signal (photons/second) per group ± SEM at the indicated time points. (Final total metastatic burden of vehicle group = $1.83 \times 10^9 \pm 1.04 \times 10^9$ p/s; PF-271 pretreatment = $4.21 \times 10^9 \pm 2.16 \times 10^9$; PF-271 post-treatment = $4.98 \times 10^8 \pm 1.73 \times 10^8$ p/s). (**C**) Representative bioluminescence images show 1 minute after injection to demonstrate dissemination through the body. Ventral and dorsal images are shown for representative mice at day 35.

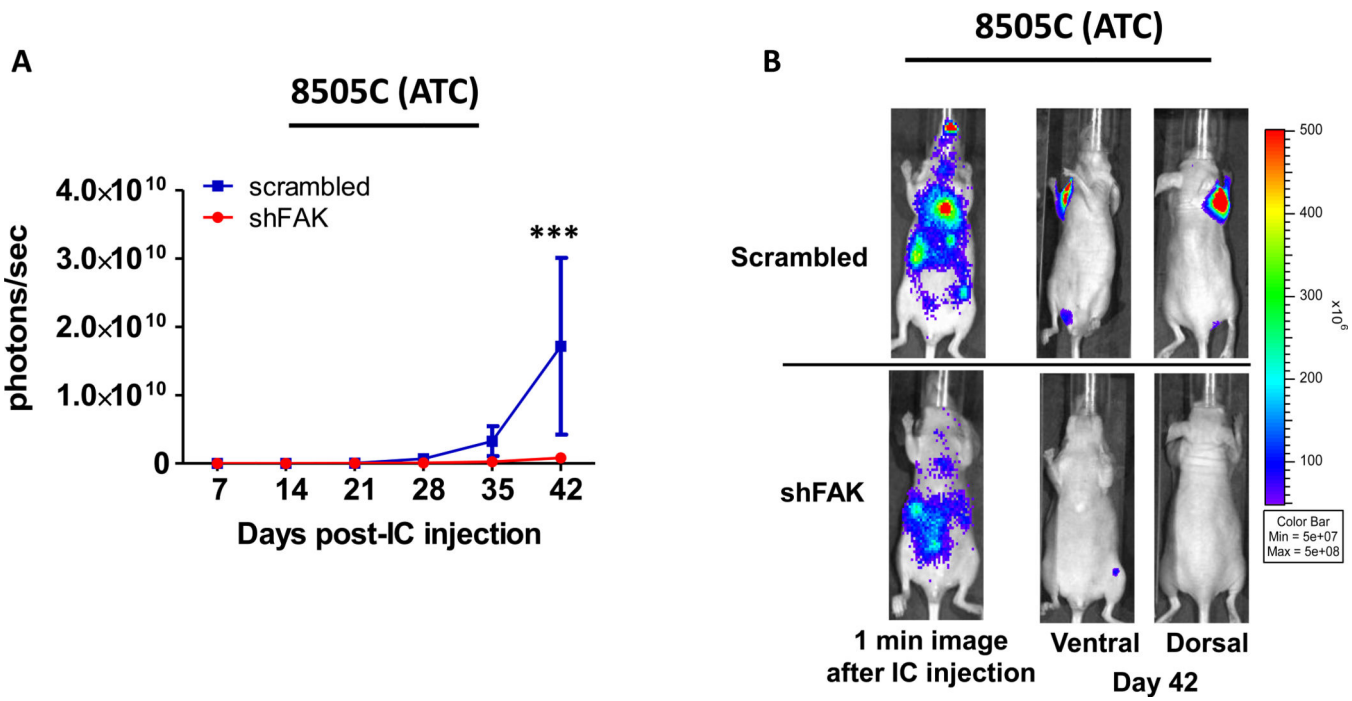

Figure 8. shFAK expression reduces metastatic tumor burden

Mice were injected with 8505C cells expressing either scrambled shRNA or shFAK. (**A**) Bioluminescence detection monitored metastatic progression over time. Results shown are mean bioluminescence signal (photons/second) per group ± SEM at the indicated time points. (Total metastatic burden: scrambled group = 1.72×1010 ± 1.29×1010 p/s; shFAK = 8.31×108 ± 2.77×108 p/s ($p \leq 0.001$; ANOVA)). (**B**) Representative bioluminescence images show 1 minute after injection to demonstrate dissemination through the body. Ventral and dorsal images are shown for representative mice at day 42.